NIH-PA Author Manuscript

NIH-PA Author Manuscript

NIH-PA Author Manuscript

Projections from Bed Nuclei of the Stria Terminalis, Dorsomedial Nucleus: Implications for Cerebral Hemisphere Integration of Neuroendocrine, Autonomic, and Drinking Responses

HONG-WEI DONG and **LARRY W. SWANSON**[*]
Department of Biological Sciences, University of Southern California, Los Angeles, California 90089-2520, USA

Abstract

The overall projection pattern of a tiny bed nuclei of the stria terminalis anteromedial group differentiation, the dorsomedial nucleus (BSTdm), was analyzed with the PHAL anterograde pathway-tracing method in rats. Many brain regions receive a relatively moderate to strong input from the BSTdm. They fall into 8 general categories: *humeral sensory-related* (subfornical organ and median preoptic nucleus—involved in initiating drinking behavior and salt appetite), *neuroendocrine system* (magnocellular: oxytocin, vasopressin; parvicellular: gonadotropin-releasing hormone, somatostatin, thyrotropin-releasing hormone, corticotropin-releasing hormone), *central autonomic control network* (central amygdalar nucleus, BST anterolateral group, descending paraventricular hypothalamic nucleus, retrochiasmatic area, ventrolateral periaqueductal gray, Barrington's nucleus), hypothalamic visceromotor pattern generator network (5 of 6 known components), *behavior control column* (ingestive: descending paraventricular nucleus; reproductive: lateral medial preoptic nucleus; defensive: anterior hypothalamic nucleus; foraging: ventral tegmental area, along with interconnected nucleus accumbens and substantia innominata), *orofacial motor control* (retrorubral area), *thalamocortical feedback loops* (paraventricular, central medial, intermediodorsal, and medial mediodorsal nuclei; nucleus reuniens), and *behavioral state control* (subparaventricular zone, ventrolateral preoptic nucleus, tuberomammillary nucleus, supramammillary nucleus, lateral habenula, and raphé nuclei). This pattern of axonal projections, and what little is known of its inputs, suggest that the BSTdm is part of a striatopallidal differentiation involved in coordinating the homeostatic and behavioral responses associated thirst and salt appetite, although clearly it may relate them to other functions as well. The BSTdm generates the densest known inputs directly to the neuroendocrine system from any part of the cerebral hemispheres.

Keywords

amygdala; bed nucleus of the stria terminalis; fluid balance; hypothalamus; sodium appetite

INTRODUCTION

As part of a systematic, high-resolution analysis of how axonal projections from the various cell groups making up the bed nuclei of the stria terminalis (BST) are organized and distributed spatially to the rest of the brain, we have already described experiments dealing with the posterior division (Dong and Swanson, 2004b), as well as with the lateral group of

[*]Correspondence to: Dr. L.W. Swanson, Hedco Neuroscience Building, 3641 Watt Way, University of Southern California, Los Angeles, California 90089-2520. Voice: (213) 740-5892 / Fax: (213) 741-0561. Email: lswanson@usc.edu.
Dr. Dong's present address is Allen Institute for Brain Science, 551 N 34th Street, Suite 200, Seattle, WA 98103.

the anterior division, also known as the anterolateral group (Dong et al., 2000, 2001b; Dong and Swanson, 2003, 2004a). This and the accompanying two papers (Dong and Swanson, 2005a,b) deal with the third major component of the BST, the medial group of the anterior division (the BST anteromedial group; BSTamg).

Viewed broadly, BST posterior division cell groups share massive, topographically organized, bidirectional connections with the medial amygdalar nucleus and other amygdalar components of the accessory olfactory system (Dong et al., 2001a; Dong and Swanson, 2004b), and they send massive, topographic projections to components of the hypothalamic behavior control column that are associated with the two basic classes of social behavior: reproductive and defensive (Dong and Swanson, 2004b). In contrast, the BST anterolateral group receives massive inputs from the central amygdalar nucleus and main olfactory system components of the amygdala (Dong et al., 2001a), and sends dense projections to the central autonomic control network, to midbrain structures positioned to modulate the expression of orofacial and locomotor somatomotor responses, and to regions of the ventral striatopallidal system associated with these midbrain structures (Dong et al., 2000, 2001b, 2003, 2004a). This projection pattern suggests BST anterolateral group involvement in the expression of ingestive (eating and drinking) behaviors and associated homeostatic mechanisms.

Unlike the BST posterior division and anterolateral group, the BSTamg receives major inputs from both the central and medial amygdalar nuclei, and from amygdalar components associated with both the main and accessory olfactory systems (Dong & Swanson, 2001a). Of special interest, previous anterograde (Swanson and Cowan, 1979; Risold et al., 1997) and retrograde (Sawchenko and Swanson, 1983; Cullinan et al., 1993; Moga and Saper, 1994; Spencer et al., 2005) pathway tracing experiments suggested that the general region of the BSTamg projects densely to specific neuroendocrine motoneuron pools in the hypothalamus (also see Swanson, 1987). However, the overall pattern of BSTamg projections has not been examined systematically with contemporary pathway tracing methods.

This paper deals with a small, clearly differentiated cell group—the dorsomedial nucleus (BSTdm)—embedded in the caudomedial end of the BSTamg. The BSTdm lies just ventral to the anterior commissure, between the undifferentiated BST anteromedial area (BSTam) and the lateral edge of the medial preoptic area. Its major inputs from "striatal" parts of the amygdalar region (McDonald, 1992; Swanson and Petrovich, 1998; Swanson, 2003) are unique, arising in ventral capsular regions of the central nucleus and in the anterodorsal part of the medial nucleus (Dong et al., 2001a). As shown here, the axonal projections of the BSTdm also differ from those of other BST anterior division components. Overall, the connectional evidence suggests that the BSTdm is involved particularly in the cerebral hemisphere coordination and regulation of neuroendocrine, autonomic, and somatic responses associated with fluid balance homeostasis, including drinking behavior and sodium appetite.

MATERIALS AND METHODS

They were identical to those described earlier (Dong and Swanson, 2003). Experiments were performed according to NIH Guidelines for the Care and Use of Laboratory Animals, and all protocols were approved by the University of Southern California Institutional Animal Care and Use Committee. The experiments described here were chosen from a collection of over 200 PHAL injections in all parts of the BST. Adult male Harlan Sprague-Dawley rats (300-350 g) received a single, stereotaxically placed iontophoretic injection of a 2.5% solution of PHAL (Vector Laboratories, Burlingame, CA), prepared in 0.1 M sodium

phosphate-buffered saline (NaPBS), pH 7.4, into various regions of the BST through a glass micropipette (15 μm tip diameter) by applying a positive current (5 μA, 7 sec on/off intervals) for 7-10 min. Animals were anesthetized for stereotaxic surgery with an equal mixture of ketamine and xylazine solutions (50 mg/ml ketamine, 10 mg xylazine/ml; 1 ml/kg body weight).

After surviving 14-16 days, the rats were deeply anesthetized with pentobarbital (40 mg/kg body weight, intraperitoneal) and perfused transcardially with 150 ml of 0.9% NaCl followed by 300 ml of ice-cold 4% paraformaldehyde in 0.1 M borate buffer (pH 9.5). Brains were removed, post-fixed overnight at 4°C in the same fixative containing 10% sucrose, and frozen. Then serial 30 μm-thick sections (1-in-4) were cut in the transverse plane on a sliding microtome. One complete series of sections was processed to detect PHAL using the immunohistochemical procedure described elsewhere (Gerfen and Sawchenko, 1984; Petrovich and Swanson, 1997). PHAL-containing cells (in the injection sites) and fibers were plotted with the aid of a camera lucida onto cytoarchitectonic drawings of adjacent thionin-stained sections, and then transferred onto a series of standard drawings of the rat brain (Swanson, 2004) with the aid of a computer (Apple, Mac PowerPC G4, Adobe Illustrator CS). Photomicrographs were taken with a CCD camera (Diagnostics Instruments, Sterling Heights, MI) or with a Wild Leitz 35 mm camera mounted on a Wild M3Z stereozoom microscope. Film was digitized with a Nikon scanner (LS-1000), and all digital files were composed, and adjusted for brightness and contrast, in Adobe Photoshop 5 using a Mac PowerPC G4. Parceling of the rat brain, the terminology for describing morphological features of PHAL-labeled axons, and mapping strategies and procedures follow Swanson (2004), unless indicated otherwise.

RESULTS

Nomenclature

The BSTdm was described originally as a "loosely arranged, relatively ill-defined nucleus that partly envelops the lateral aspect of the parastrial nucleus" (Ju and Swanson, 1989), and no unique, distinguishing, chemoarchitectonic features were identified at the time (Ju et al., 1989). Our PHAL analysis of BST connections, accompanied by a great deal more cytoarchitectonic examination in over 200 brains, provides the basis for proposing a revised definition of BSTdm boundaries. First, the rostral tongue of the original BSTdm (Atlas Levels 16-19; Swanson 1998-1999) is assigned to the BSTam. The connectional evidence for this reassignment is presented briefly in the Results section, and in more detail in the accompanying paper (Dong and Swanson, 2005b). It is based on observations that PHAL injections involving the rostral tongue of the original BSTdm, but not its caudal end, do not label the projection pattern described below, but instead label the pattern characteristic for the BSTam (see experiments BST13, 114, and 134 illustrated in Dong and Swanson, 2004b). And second, the caudal end of the original BST dorsolateral nucleus (Atlas Levels 21; Swanson 1998-1999) is now assigned to the BSTdm, based on the evidence provided by injection sites illustrated in Figure 1 (below). Based on these revisions, the current borders of the BSTdm identify a more compact, better-defined cell group restricted to Atlas Levels 20-21 in Swanson (1998-1999). This simplified parcellation is adopted in Swanson (2004).

Injection sites

In our collection of PHAL experiments involving the BST, only three injection sites (experiments BST116, 148, and 155) are centered in the BSTdm as defined here, and none of them are confined entirely within its borders (Fig. 1). There are always at least a few PHAL-labeled neurons in adjacent BST cell groups (especially the adjacent anteromedial area and magnocellular nucleus), and in the parastrial nucleus of the hypothalamic preoptic

region (Figs. 1 and 2). Because of the BSTdm's tiny volume (about $350 \times 400 \times 200$ μm; rostrocaudal by mediolateral by dorsoventral) and irregular shape it is probably not possible to obtain stereotaxically placed PHAL injections confined entirely within the cell group's borders. In addition, the dendrites of neurons in adjacent cell groups (e.g., the BST magnocellular nucleus; Dong and Swanson, 2005a) can extend into the BSTdm, and it is well known that PHAL is avidly incorporated by dendrites (Gerfen and Sawchenko, 1984). However, as controls for this spread or contamination, we have analyzed the projections of the adjacent cell groups, as described below. The overall pattern of axonal projections labeled by PHAL injections centered in the BSTdm is clearly distinct from those labeled by injections centered in adjacent cell groups. Obviously, the following results simply constitute a reliable starting point for more detailed and incisive structural and functional characterization of BSTdm projections with retrograde tracer, single-cell labeling, histochemical, and neurophysiological methods.

PHAL labeling in experiment BST116 is illustrated in detail because its injection site had the least spread to adjacent cell groups (Figs. 1 and 2). However, the overall projection pattern labeled here is indistinguishable from that labeled in the other two experiments with a PHAL injection centered in the BSTdm.

BSTdm projections

PHAL-labeled axons arising from the BSTdm follow at least seven distinct pathways to generate over 80 recognizable terminal fields in the ipsilateral basal endbrain (telencephalon, cerebral hemisphere), interbrain (diencephalon), and lower brainstem (midbrain and hindbrain; Fig. 3). The distribution of PHAL-labeled axons in experiment BST116 was plotted onto a series of reference rat brain templates (Fig. 4).

Local projections within the BST—In the BST anterior division, the BSTdm moderately to densely innervates the BSTam and caudoventral region of the anterolateral area, and the fusiform, rhomboid, and ventral nuclei—whereas the rostral two-thirds of the anterolateral area and the caudodorsal end of the anteromedial area, along with the oval and juxtacapsular nuclei, receive only sparse inputs at best. In the BST posterior division, only the interfascicular nucleus and ventral regions of the transverse nucleus receive significant inputs from the BSTdm.

Several obvious pathways contribute to these intra-BST terminal plexuses. First, many PHAL-labeled axons from the BSTdm injection site extend rostrally, dorsal and ventral to the anterior commissure, to merge in the rostrodorsal tip of the anteromedial area (Fig. 4D-H). Dorsal to the anterior commissure these fibers present abundant terminal boutons along the entire length of the anteromedial area (Figs. 4D-G and 5A), except very caudally where, along with the rostral anterolateral area and the oval and juxtacapsular nuclei (Fig. 4C-G), only a few scattered axons are observed. Ventral to the anterior commissure PHAL-labeled axons display many short branches and abundant boutons in the anteromedial area and fusiform nucleus (Figs. 4D-G and 5B). Along this rostral projection many PHAL-labeled axons leave the BST to enter adjacent regions (see next Section).

The second pathway from the BSTdm injection site extends laterally through the magnocellular and ventral nuclei, and ventral regions of the anteromedial area, to caudal levels of the anterolateral area—where it splits into two bundles (Fig. 4H,I). One small bundle ascends through the rhomboid nucleus to join the stria terminalis; the other, larger bundle courses ventrally into the substantia innominata and its ansa peduncularis. Before leaving, this pathway generates moderate numbers of terminal boutons in the rhomboid nucleus and caudoventral regions of the anterolateral area (Fig. 4H,I).

The largest pathway from the BSTdm injection site extends ventrally through the magnocellular and ventral nuclei to the medial and lateral preoptic areas, and adjacent dorsomedial region of the substantia innominata (Figs. 4H-J and 5C). Before leaving the BST these axons generate abundant boutons in the magnocellular and ventral nuclei (Fig. 4H-J), indicating that they receive the densest intra-BST inputs from the BSTdm.

Finally, many axons from the BSTdm injection site extend caudally into the BST posterior division, where moderate numbers of fibers with boutons are observed in the interfascicular nucleus and ventral region of the transverse nucleus; the principal nucleus contains only scattered fibers (Fig. 4J). Many of these fibers continue on into the substantia innominata, rostral end of the lateral hypothalamic area, and medial preoptic area—where they join the medial forebrain bundle or the ventral and lateral propriohypothalamic pathways (next Section).

Rostral projections from the BSTdm—On leaving the BST rostrally directed fibers provide substantial inputs to several adjacent brain structures. Dorsal to the anterior commissure, a few BSTdm axons leave the BST to enter the lateral septal complex directly (Fig. 4D-G). Ventral to the anterior commissure, many axons extend ventrally and generate moderate to dense inputs in rostral levels of the substantial innominata, the lateral preoptic area, and the parastrial and anterodorsal preoptic nuclei (Figs. 4E-G and 5B). Then, most of these rostrally directed axons arch dorsally and laterally around the rostromedial edge of the anterior commissure to enter the lateral septal complex (Fig. 4A-G). Many rostrally directed fibers from the BST also extend directly into the nucleus accumbens.

Rostrally directed BSTdm axons thus provide major inputs to two regions: the nucleus accumbens and lateral septal nucleus. In the former, the densest terminals are observed in dorsal, medial, and ventral regions of the caudal or septal pole (Fig. 4C), tending to avoid the more central "core" (Fig. 4C). More rostrally, PHAL labeling decreases dramatically (Fig. 4A,B) and only a few axons and terminals are distributed sparsely in ventromedial "shell" regions of the nucleus accumbens.

In the lateral septal nucleus, the BSTdm provides substantial inputs to several distinct components of the rostral part, in the medial (LSrm, r.m.v.r, r.m.d) and dorsolateral (r.dl.m.v, r.dl.m.d, r.dl.l.d) zones (Fig. 4A-G). The rest of the rostral part (including the LSr.vl.v) and the caudal part (including LSc.v.l.d and LSc.v.m.v) receive only light inputs, and the ventral part contains scattered fibers at best (Fig. 4A-G).

Finally, a small number of axons leave the rostral end of the lateral septal nucleus to terminate in the infralimbic, prelimbic, and dorsal and ventral agranular insular cortical areas (Fig. 4A,B).

Ascending stria terminalis and ansa peduncularis pathways to temporal region—Only a few axons from the BSTdm injection site follow the stria terminalis to the amygdalar region (Figs. 3 and 4K-S). Along the way a small, distinct terminal field is observed dorsolaterally in the stria and immediately adjacent regions of the caudoputamen, at the level of the caudal tip of the anterodorsal thalamic nucleus (Fig. 4O). Our material does not allow distinction between amygdalar fibers arriving via the stria terminalis and ansa peduncularis because they intermingle.

Most PHAL-labeled BSTdm axons reach the amygdalar region through the ventrally directed ansa peduncularis (Fig. 3). Along the way they generate abundant boutons of passage and terminal boutons in the caudal substantia innominata (Fig. 4H-O).

The central amygdalar nucleus appears to receive the densest input (Fig. 3). Abundant PHAL-labeled axons branch profusely and generate abundant terminal boutons in the medial part and in ventral regions of the capsular part, whereas lateral regions of the capsular part are virtually avoided (Figs. 4K-Q and 5D). Small numbers of fibers and terminals are also found in the anterior amygdalar area, anterodorsal part of the medial nucleus, and anterior basomedial nucleus (Fig. 4L-P).

BSTdm projections to hypothalamus—Descending BSTdm axons follow the periventricular, ventral, and lateral propriohypothalamic pathways, and the medial forebrain bundle, to the medially subjacent hypothalamus. Some axons in the medial forebrain bundle extend into the thalamus, whereas axons remaining in the caudal hypothalamus continue on to the midbrain and hindbrain. A few axons course through the stria medullaris to the thalamus (Fig. 3). The pattern of BSTdm inputs to the hypothalamus is exceptionally complex, and unique.

<u>Periventricular propriohypothalamic pathway (of Thompson and Swanson, 2003):</u> Many PHAL-labeled axons from the BSTdm injection site extend dorsomedially into the median preoptic nucleus, ventral to the crossing of the anterior commissure (Fig. 4H,I), before ascending and descending to innervate a variety of structures in the hypothalamic periventricular region of Thompson and Swanson (2003).

The ascending fibers generate an extremely dense terminal plexus throughout the median preoptic nucleus, bilaterally with an ipsilateral predominance (Figs. 4E-I and 6A,D). Rostroventrally PHAL-labeled axons generate abundant branches and boutons surrounding the vascular organ of the lamina terminalis (Figs. 4D,E and 6A), and some invade the lamina terminalis itself (Fig. 6A,B,C).

Other fibers in the median preoptic nucleus extend dorsally and caudally, eventually to enter the subfornical organ (Fig. 4H-K), where they branch infrequently but generate abundant boutons, especially peripherally (Figs. 4J,K and 6E).

Descending periventricular fibers course through and innervate moderately to densely the preoptic, anterior, and intermediate parts of the periventricular nucleus (Fig. 4H-S), whereas the arcuate (Fig. 4N-R) and posterior periventricular (Fig. 4S-U) nuclei are sparsely innervated.

However, the densest BSTdm terminal field associated with this pathway is established in all three divisions (parvicellular, magnocellular, and descending) of the paraventricular nucleus. All three parts of the parvicellular neuroendocrine division (anterior, dorsal medial, and periventricular) contain a dense terminal plexus (Figs. 4J-O and 7A-G), although it is lightest in intermediate regions of the dorsal medial part where neuroendocrine CRH secretomotoneurons are centered (Swanson et al., 1983) (Figs. 4N and 7E,F). Based on our collection of over 200 PHAL experiments, the densest BST input to the paraventricular magnocellular neuroendocrine division arises in the BSTdm. The anterior magnocellular part (Figs. 4J and 7A) and medial zone of the posterior magnocellular part (Figs. 4M and 7C) are heavily invested with branches and boutons, and in the lateral zone of the posterior magnocellular part this plexus tends to lie peripherally (Figs. 4N and 7C,D), although scattered fibers and terminals extend more centrally (Figs. 4N and 7C,D). This distribution is consistent with a predominant innervation of magnocellular oxytocinergic neuroendocrine neurons (Dierickx, 1980). The PVH descending division actually contains the densest input of the three, and it distributes to all four parts. Most of its fibers appear to arrive via the medial forebrain bundle.

Many periventricular fibers also course through and generate branches and boutons in the subparaventricular zone (Fig. 4L-O) and some continue into the dorsomedial nucleus (Fig. 4PR), although most inputs to the latter appear to enter via the medial forebrain bundle.

<u>Ventral propriohypothalamic pathway:</u> As mentioned, abundant PHAL-labeled BSTdm axons enter the medial preoptic area and join the ventral propriohypothalamic pathway as defined by Thompson and Swanson (2003) (Fig. 4H,I). Initially they generate extremely dense branches and boutons in the medial preoptic area and adjacent rostral pole of the anterior hypothalamic area (Figs. 4H-K and 5B). Many axons also extend medially to generate a moderate input to the lateral part of the medial preoptic nucleus (Figs. 4H-J and 5B), as well as dorsally to innervate the lateral hypothalamic area, juxtaparaventricular region (Fig. 4K-N).

Most PHAL-labeled axons in the medial preoptic area course ventrally and then near the base of the brain turn to extend rostrally and caudally.

Ascending fibers course through the medial preoptic area, generating numerous branches and boutons in the medial preoptic area and two cell groups embedded within it: the anteroventral preoptic nucleus and rostral tip of the medial preoptic nucleus (Fig. 4D-H). A few bouton-laden axons also invade peripheral regions of the anteroventral periventricular nucleus (Fig. 4F,G), indicating it is innervated as well. Rostrally this group of axons mixes extensively with those in the ascending periventricular pathway in and around the median preoptic nucleus (Figs. 4D-G and 5A). A few axons with terminal boutons are also observed in the suprachiasmatic preoptic nucleus (Fig. 4F-H).

Most ventral propriohypothalamic fibers from the BSTdm descend (Fig. 4H-K). Many of them join the pathway after traveling through (and innervating) the anterior hypothalamic nucleus and immediately adjacent regions of the lateral hypothalamic area (Fig. 4L-N). PHAL-labeled axons in the ventral pathway essentially course between the medial hypothalamic nuclei and the base of the brain, although this pathway extends laterally and somewhat dorsally to include ventral regions of the lateral propriohypothalamic pathway. Many axons here resemble fibers of passage, although considerable boutons of passage nevertheless are present, so that distinct terminal fields are present in ventral regions of the lateral hypothalamic area ventral to the fornix, specifically in the intermediate tuberal nucleus, and in the juxtaventromedial region (ventral zone) and subfornical region (posterior zone) (Fig. 4P-S).

A number of other distinct terminal fields arising from the ventral pathway are also observed. At preoptic and anterior hypothalamic levels fibers extend laterally, dorsal to the optic tract, to innervate the supraoptic nucleus (Figs. 4H-N and 8A,B). Compact, dense accumulations of fibers with abundant boutons are observed ventrally in the supraoptic nucleus (Fig. 8A), along with distinct terminal arbors dorsally (Fig. 8B). Many fibers also generate terminals in the anterior region (ventral zone) of the lateral hypothalamic area, immediately dorsal to the supraoptic nucleus (Figs. 4I-M and 8A,B). More caudally, laterally directed axons with branches and boutons extend through and to ventral regions of the lateral hypothalamic area near the optic tract, eventually to reach the amygdalar region (Fig. 4N-P).

At anterior hypothalamic levels many fibers in the ventral path turn medially to branch and generate boutons in seemingly undifferentiated regions of the anterior hypothalamic area surrounding the rostral end of the suprachiasmatic nucleus (Fig. 4I,J), and some fibers even enter the later and display prominent boutons (Fig. 4I-L). More caudally, many axons generate branches and terminal boutons in the retrochiasmatic area (Fig. 4L,M), and some

extend medially through the supraoptic commissure system to the contralateral side of the brain, where they provide scattered fibers in the anterior hypothalamic nucleus, and distinct terminal fields in the supraoptic nucleus (Fig. 4L,M).

Other distinct BSTdm terminal fields are observed in certain readily identifiable clusters of the accessory supraoptic nucleus, particularly near blood vessels in regions dorsal to and even within the optic tract (see Fig. 8C'; Peterson, 1966;Duan and Ju, 1998;Khan et al., 1999). PHAL-labeled axons penetrate through these magnocellular neurosecretory neuron clusters and display many boutons (Fig. 8C).

Axons in the ventral propriohypothalamic pathway begin to ramify and generate more terminals at the level of the caudal end of the paraventricular nucleus (Fig. 4O). As described above, many axons arch dorsomedially and provide extremely dense terminal fields in intermediate tuberal nucleus and dorsally adjacent territories of the lateral hypothalamic area's juxtaventromedial region (ventral zone) and subfornical region (posterior zone) (Figs. 4O-S and 9A). This dense terminal field extends dorsally to intermingle with a plexus generated by the medial forebrain bundle proper (see below) in regions just lateral and medial to the fornix (Fig. 4P-R). More caudally, some of these axons contribute inputs to the ventral part of the dorsomedial nucleus and the posterior nucleus (Fig. 4P-T).

Near the ventral surface of the brain at these levels a few axons extend laterally into the retrochiasmatic part of the supraoptic nucleus, where they display many prominent boutons among the magnocellular neurosecretory neurons (Fig. 4O,P). Some axons with a few terminals also extend medially into the ventrolateral part of the ventromedial nucleus (Fig. 4P-R). The remaining fibers proceed caudally, branching occasionally and generating a few terminals in the ventral tuberomammillary nucleus and terete subnucleus of the tuberal nucleus, just lateral to the ventral premammillary nucleus (Fig. 4T,U). They proceed caudally in the ventral, fibrous "capsule" of the mammillary body and then arch dorsomedially through the medial part of the supramammillary nucleus and posterior hypothalamic nucleus toward the periaqueductal gray (Fig. 4V,W). The dendrites of many medial mammillary nucleus neurons extend into the ventral capsular region (Cajal, 1995), which contains many terminal boutons from the BSTdm.

Medial forebrain bundle: Many PHAL-labeled axons from the BSTdm injection site course through dorsal regions of the substantia innominata, medial regions of the lateral preoptic area, and anterior region of the lateral hypothalamic area to join the medial forebrain bundle (Figs. 4H-K and 5C). At preoptic levels abundant branching and bouton generation occur, indicating that the three regions are densely innervated (Fig. 4H-K).

A distinct terminal field near the ventromedial corner of the lateral preoptic area (Figs. 4H and 5C) is generated in the region of the sleep-related ventrolateral preoptic nucleus (Sherin et al., 1996;Chou et al., 2002;Lu et al., 2002).

At the level of the anterior hypothalamic nucleus most BSTdm axons descend in the medial half of the lateral hypothalamic area, where they are cut in cross-section and appear to be fibers of passage (Fig. 4K-N). However, there are many boutons of passage along this route, and axons frequently arch dorsally into the thalamus (Fig. 4L-N).

As this major descending bundle reaches the caudal end of the anterior hypothalamic nucleus many fibers extend medially through the lateral parvicellular part (lateral wing) of the paraventricular nucleus (Figs. 4O and 7G). These transverse fibers display numerous boutons of passage along their length and generate a dense terminal plexus in the lateral tip (the tiny forniceal part) and in the medial segment of the lateral parvicellular part (Figs. 4O

and 7G). Extending rostrally from the medial segment, this dense terminal plexus splits into dorsal and ventral limbs, contributing strong inputs to the dorsal parvicellular (dorsal cap) and ventral medial parvicellular parts of the paraventricular descending division (Figs. 4N and 7C-F). It is not clear whether this fiber system innervates other parts of the paraventricular nucleus as well.

Just caudal to the paraventricular nucleus, medial forebrain bundle fibers generate an extremely dense terminal plexus in the suprafornical region of the lateral hypothalamic area, between the zona incerta and fornix (Figs. 4P-R and 9A). Lateral and medial to the fornix, some of these fibers intermix with those extending dorsally from the ventral propriohypothalamic pathway described above. Many axons also extend medially to provide very dense inputs to the juxtadorsomedial region of the lateral hypothalamic area, and to the anterior and ventral parts of the dorsomedial nucleus; the posterior part of the dorsomedial nucleus contains only scattered axons (Figs. 4P-R and 9A).

Near the caudal end of the ventromedial nucleus some PHAL-labeled axons leave the medial forebrain bundle to enter and very densely innervate the posterior hypothalamic nucleus (Fig. 4Q-U). Remaining axons in this dorsal branch either extend farther dorsally into the thalamus (Fig. 4Q-U) or arch caudally into the periaqueductal gray (Fig. 4V).

Axons in the medial forebrain bundle proper continue caudally in the posterior region of the lateral hypothalamic area (Fig. 4T,U) where they branch occasionally and generate a few boutons—but tend to avoid the parasubthalamic nucleus, which is densely innervated by the BST rhomboid nucleus and other BST anterolateral cell groups (see Dong and Swanson, 2003, 2004a).

Near the caudal end of the hypothalamus many PHAL-labeled axons turn medially to generate a strong input to the lateral supramammillary nucleus (Fig. 4V) and some even extend more medially to innervate bilaterally the medial supramammillary nucleus (Fig. 4V).

Remaining axons in the caudal end of the lateral hypothalamic area (Fig. 4V) descend into the midbrain and then hindbrain.

BSTdm inputs to thalamus—Throughout their descending course through the medial forebrain bundle, some fibers arch medially and then dorsally into the thalamus (Fig. 4J-U). Most rostrally they enter the paraventricular thalamic nucleus directly and present only a few boutons (Fig. 4J,K). These fibers tend to extend caudally in the dorsal periventricular bundle centered in the paraventricular nucleus, a course taken by axons from other BST cell groups (such as the rhomboid nucleus; Dong and Swanson, 2003). All along anterior and tuberal hypothalamic levels scattered fibers leave the medial forebrain bundle to arch medially through the zona incerta, and then more caudally through the posterior hypothalamic nucleus, to enter the midline thalamic nuclei (Fig. 4L-R). However, the largest number of mediodorsally arching fibers leave the medial forebrain bundle at the level of the caudal third of the paraventricular thalamic nucleus, arching initially through the posterior hypothalamic nucleus (which is heavily innervated, see above) and then through the central medial and intermediodorsal nuclei to end in caudal regions of the paraventricular nucleus (Fig. 4S-U). Thus, the BSTdm provides its densest thalamic inputs to caudal regions of the paraventricular nucleus, which is densely innervated bilaterally, with an ipsilateral predominance (Fig. 4O-U). Many branched, bouton-laden fibers are also observed in the central medial nucleus, intermediodorsal nucleus, and medial part of the mediodorsal nucleus (Fig. 4S-U). More rostrally, PHAL-labeled axons regularly display terminal boutons

in several parts of the nucleus reuniens (Fig. 4L-R), including the medial, lateral, and ventral parts of the rostral division, and the dorsal and posterior parts of the caudal division.

In contrast to other parts of the BST, the BSTdm sends an obvious group of axons through the stria medullaris to the thalamus (Fig. 3). PHAL-labeled axons join the stria at the rostral pole of the thalamus (Fig. 4J-L), and then extend caudally as unbranched fibers of passage (Fig. 4M-R). Along the way they send a few terminals to the anterodorsal nucleus (Fig. 4O) before beginning to branch and generate boutons in the caudal half of the lateral habenula (Fig. 4S-U). The terminal plexus is most dense in peripheral regions of the caudal tip and in adjacent medial regions of the parafascicular nucleus (Fig. 4U). A few axons also extend into the medial habenula (Fig. 4U). This pathway appears to end as a moderate terminal field in the precommissural nucleus of the periaqueductal gray (Fig 4V).

BSTdm projections to lower brainstem—Near the interbrain/midbrain junction the BSTdm projection splits. One part ascends from the caudal hypothalamus to the midbrain periventricular system in the periaqueductal gray and the other is simply a caudal extension of the medial forebrain bundle. The latter also gives off a median branch that courses through the raphé nuclei (Fig. 3).

Midbrain periventricular pathway: Initially these axons generate abundant, prominent boutons in the medial division, and in adjacent regions of the rostromedial division, of the periaqueductal gray (Fig. 4V,W). Then they turn abruptly and descend nearly perpendicular to the transverse plane of section. These fibers course adjacent to the aqueduct as a fairly compact bundle generating few branches but many boutons of passage and terminal boutons in the medial division and adjacent regions of the rostromedial division—and commissural nucleus—of the periaqueductal gray (Fig. V-X) before ending in the pontine central gray (Fig. 4Y-CC). Along this route a few axons turn dorsally to generate small terminal fields in the periaqueductal gray dorsal division (Fig. 4Y-CC). Some of these fibers continue dorsally to enter deeper layers of the superior colliculus (Fig. 4W-BB).

Medial forebrain bundle: These axons extend from the posterior region of the lateral hypothalamic area into the ventral tegmental area (Fig. 4V,W), where they branch infrequently but generate many boutons to provide a relatively moderate input (Fig. 4W-Y). One small group of BSTdm axons leaves the ventral tegmental area medially to enter the interfascicular, rostral linear, and central nuclei of the raphé (Fig. 4X-AA), where they generate sparse boutons. A small extension of this pathway arches dorsally to innervate the dorsal nucleus of the raphé (Fig. 4Z-BB). The remaining fibers continue caudally through the superior central nucleus (median nucleus of the raphé) and tegmental reticular nucleus to end in the medullary nuclei of the raphé and adjacent regions of the reticular formation (Fig. 4Z-KK). These fibers display few branches but many terminal boutons in the nucleus raphé magnus (Fig. 4EE-II) and nucleus raphé pallidus (Fig. 4HH-JJ) before ending in the nucleus raphé obscurus (Fig. 4KK).

Lateral course of the medial forebrain bundle: Most BSTdm axons from the ventral tegmental area follow this classic route through the midbrain (Fig. 3). Initially they turn laterally and travel through a region between the substantia nigra and medial lemniscus (including the caudal end of the zona incerta; see Fig. 4W-Y). After providing a light input to the parvicellular part of the subparafascicular thalamic nucleus (Fig. 4W,X), the vast majority of axons course through several components of the midbrain reticular nucleus before arching medially into the periaqueductal gray at about the level of the trochlear nucleus (Fig. 4Y-BB). Along the way these fibers branch frequently and generate abundant boutons in the retrorubral area and adjacent regions of the midbrain reticular nucleus, and a few axons also end in the pedunculopontine nucleus (Fig. 4BB-CC).

PHAL-labeled axons in the three pathways just described converge on the caudal periaqueductal gray (Fig. 3) where there is an extremely dense terminal plexus extending through the medial and ventrolateral divisions (Figs. 4Z-BB and 9B). There is also a light input to the periaqueductal gray dorsal division, and substantial terminal fields are observed in the laterodorsal tegmental nucleus and dorsal nucleus of the raphé (Fig. 4Z-BB).

The remaining fibers continue caudally into the pontine central gray (Fig. 4DD), where they tend to funnel into a restricted region immediately medial to the root of the trochlear nerve, and then more caudally, just medial to the locus ceruleus (Fig. 4DD,EE). After generating abundant boutons in this region of the pontine central gray these axons dive ventrally to end in Barrington's nucleus, which is heavily innervated by an extremely dense terminal field (Figs. 4DD and 10A). This terminal field is remarkably confined to Barrington's nucleus, leaving immediately adjacent regions almost devoid of PHAL labeling (Fig. 10A).

Near the caudal end of the pontine central gray a few labeled axons turn laterally to enter the parabrachial nucleus, where there is a light terminal field in the central part of the lateral division (Fig. 4CC-FF). Furthermore, a number of fibers extend ventrally through the sublaterodorsal nucleus and pedunculopontine nucleus into the pontine reticular nucleus (Fig. 4DD-GG). They branch little and generate many small boutons in ventral regions of the caudal pontine reticular nucleus (Fig. 4EE-GG). More caudally, these axons travel through the ventral medulla, where they generate many boutons in ventromedial regions of the gigantocellular reticular nucleus (Fig. 4HH,KK), ventromedial regions of the magnocellular reticular nucleus near the medial lemniscus (Fig. 4JJ,KK), lateral part of the paragigantocellular reticular nucleus and parvicellular reticular nucleus (Fig. 4JJ,KK), and finally end in a ventrolateral region of the ventral medullary reticular nucleus that contains the A1 noradrenergic cell group (Fig. 4LL). These fibers may also contribute inputs to the hindbrain raphé nuclei (Fig. 4FF-KK).

Contralateral projections

As already described, projections from BSTdm to midline brain structures (such as the median preoptic nucleus, subfornical organ, retrochiasmatic area, midline thalamic nuclei, and raphé nuclei) are bilateral with an ipsilateral predominance. Typically the contralateral side is innervated by fibers that simply cross the midline from ipsilateral regions of the particular midline structure.

The BSTdm also generates light contralateral projections to many other brain regions, and these projections tend to mirror the ipsilateral projection pattern (Fig. 3).

At the injection site level, a few axons course immediately dorsal and ventral to the anterior commissure to reach the contralateral side where they generate scattered terminals in the BST and lateral septal nucleus (Fig. 4D-J). A few of these axons follow the contralateral ansa peduncularis to the medial part of the central amygdalar nucleus (Fig. 4J-O).

Along the length of the hypothalamus scattered axons cross the midline dorsal and ventral to the third ventricle. They generate a few terminals in the contralateral periventricular, paraventricular, and supraoptic nuclei; the medial and lateral preoptic areas; the lateral medial preoptic, anterior hypothalamic, and dorsomedial nuclei; and the lateral hypothalamic area (Fig. 4D-U). Denser contralateral projections are found in the posterior hypothalamic and supramammillary nuclei (Fig. 4Q-W).

From the posterior hypothalamic nucleus, a substantial number of axons enter the contralateral periaqueductal gray (Fig. 4V,W) and follow the dorsal periventricular system toward the pontine central gray. Along the way, these BSTdm axons generate substantial

boutons in the medial and rostromedial periaqueductal gray divisions, and in its commissural nucleus, before ending in the ventrolateral division (Fig. 4V-CC). A few axons with terminal boutons are also observed in the contralateral pontine central gray and Barrington's nucleus (Fig. 4DD-FF).

A small number of labeled BSTdm axons in the contralateral medial forebrain bundle descend through the ventral tegmental area, retrorubral area, and other parts of the midbrain reticular nucleus (Fig. 4W-BB), where they generate terminal boutons. Finally, there are a few labeled axons in pontine and medullary regions of the contralateral reticular formation (Fig. 4FF-JJ).

Control injections

It is important to reiterate that none of our PHAL injections labeled only neurons confined entirely within the borders of the BSTdm (Figs. 1 and 2)—a few neurons were always labeled in adjacent regions. To clarify whether some of the more lightly labeled projections illustrated in Figures 3 and 4 might be characteristic only of the adjacent regions, it is important to analyze the results of PHAL experiments centered in these adjacent regions. It is also possible, of course, that certain projections arise from a neuronal cell type(s) distributed in the BSTdm as well as in an adjacent region(s). The latter possibility can only be examined definitively at this time with retrograde tracer experiments, but it is obvious from examining Figure 3 that a retrograde tracer analysis of most BSTdm projections is not practical. For an analysis of regions adjacent to the BSTdm, the following material is available: 10 PHAL injections centered in ventral regions of the BSTam that are laterally adjacent to the BSTdm, three small injections restricted to the BST magnocellular nucleus immediately ventral to the BSTdm, and one injection centered in the rostromedially adjacent parastrial nucleus. The overall projection pattern labeled from each of these three regions is quite distinct from that labeled from the BSTdm.

Parastrial nucleus—The overall projections of the parastrial nucleus, based on PHAL analysis, have been described previously (Simerly and Swanson, 1988; Thompson and Swanson, 2003); here, clear differences with the BSTdm are emphasized. First, it is important to note that the parastrial nucleus receives little input from the stria terminalis/ amygdalar region (Simerly et al., 1984; Dong et al., 2001a), and does not project significantly to the central amygdalar nucleus (see Thompson and Swanson, 2003)—which receives a clear input from the BSTdm, and all other components of the BST anterior division (Dong et al., 2000, 2001b; Dong and Swanson, 2003, 2004a, 2005a,b). These are the most characteristic differences between the parastrial nucleus and the BST.

Second, compared to the BSTdm the parastrial nucleus projects more substantially to the lateral septal nucleus, which is particularly obvious in the LSr.m.v.c. Third, projections from parastrial nucleus to lower brainstem are very different (Thompson and Swanson, 2003), coursing almost exclusively through the dorsal periventricular system and median branch of the medial forebrain bundle. Thus, it does not significantly innervate the retrorubral area and adjacent regions of the midbrain reticular nucleus, and inputs to the periaqueductal gray's ventrolateral division and to Barrington's nucleus are light—all of which are densely innervated by the BSTdm. In addition, the parastrial nucleus does not send detectable projections to the medulla, unlike the BSTdm.

And fourth, the parastrial nucleus and BSTdm share many common targets in the hypothalamus, although there are subtle differences. Axons from both nuclei course through the periventricular, ventral, and lateral propriohypothalamic pathways, but only axons from the BSTdm course through the medial forebrain bundle proper. Therefore, the BSTdm provides much denser projections to the suprafornical region of the lateral hypothalamic

area. In the periventricular region, the BSTdm and parastrial nucleus both project densely to the anterior and intermediate regions of the periventricular nucleus, and to the parvicellular and magnocellular neuroendocrine divisions of the paraventricular nucleus. For example, the BSTdm projects to the anterodorsal preoptic, anterior hypothalamic, and lateral supramammillary nuclei, whereas the parastrial nucleus does not.

Ventral BSTam—The projections of this region are analyzed in the accompanying paper (Dong and Swanson, 2005b). In brief, they are clearly distinct from those of the BSTdm, especially in two domains. First, in the hypothalamus the BSTam sends very dense projections to the medial part of the medial preoptic nucleus, arcuate nucleus, and posterior region of the periventricular nucleus—but almost none to the median preoptic nucleus and descending division of the paraventricular nucleus. And second, in the lower brainstem the BSTam provides only light inputs to the retrorubral area and other regions of the midbrain reticular nucleus, and to Barrington's nucleus; and almost no inputs to the medullary components of the raphé and reticular nuclei, which receive obvious inputs from the BSTdm.

BST magnocellular nucleus—The projections of this nucleus are also analyzed in an accompanying paper (Dong and Swanson, 2005a). The PHAL evidence suggests that the overall projection pattern of the BSTmg is essentially a subset of that generated by the BSTdm (also see Table 1 in Dong and Swanson 2005b). However, the two cell groups are so small and intimately related—with dendrites from each extending into the other—that additional methods need to be applied to the problem. For example, in two instances where retrograde tracers have been injected—in Barrington's nucleus (Valentino et al., 1994) and in the lateral parvicellular part of the paraventricular nucleus (Lori Gorton and Alan G. Watts, personal communication)—labeling has been observed in both regions.

DISCUSSION

There is virtually no published neuroanatomical data on the projections of the BSTdm proper with either anterograde or retrograde tracing methods. Previous anterograde tracing studies used very large injections, most of which seem to have missed the BSTdm (e.g., Conrad and Pfaff, 1976; Swanson, 1976; Swanson and Cowan, 1979; van der Kooy et al., 1984; Holstege et al., 1985), and most retrograde tracing studies did not parcel the BST carefully. Our PHAL data indicates that the pattern of axonal projection from the BSTdm is exceptionally complex, following at least 7 pathways to more than 80 recognizable terminal fields in the ipsilateral side of the brain—and that there is a generally much lighter contralateral projection that essentially mirrors the ipsilateral pattern (Fig. 3). As already discussed for the similarly complex projection pattern generated by the BST rhomboid nucleus (Dong and Swanson, 2003), this situation presents formidable problems for further structural and functional analysis. On the other hand, the terminal fields innervated by the BSTdm fall into a number of fairly obvious functional categories that suggest interesting possibilities.

Functional implications: projection targets

Brain regions directly innervated in a substantial way by the BSTdm can be sorted, at least provisionally, into seven functional categories: viscerosensory, visceromotor (autonomic and neuroendocrine), rostral behavior control column (goal oriented behavior), caudal behavior control column (foraging/exploratory behavior), orofacial motor, thalamocortical loops, and behavioral state control.

Viscerosensory-related—The first category here concerns especially the ascending "relay" of classical viscerosensory information through the lateral division of the parabrachial nucleus (Herbert et al., 1990), which in turn projects to many brain regions involved in autonomic and neuroendocrine activities (see Bester et al., 1997). Most BSTdm input to the parabrachial nucleus is concentrated in the central part of the lateral division, whose connections suggest that it is involved primarily in the conduction of viscerosensory information from the medial nucleus of the solitary tract (see Alden et al., 1994).

The second category concerns two "humerosensory" brain regions, the subfornical organ and vascular organ of the lamina terminalis/median preoptic nucleus region. The former has receptors for circulating angiotensin II, as well as osmoreceptors (see Lind et al., 1984; Swanson and Lind, 1986; Denton et al., 1996; Johnson and Thunhorst, 1997; Fitzsimons, 1998; McKinley et al., 1996, 1998), and the latter has osmoreceptors (Denton et al., 1996; Bourque and Oliet, 1997; Johnson and Thunhorst, 1997; Fitzsimons, 1998; McKinley et al., 1996, 1998). The role of these two regions in drinking behavior and sodium appetite is documented in the literature just cited, and the neural circuitry underlying this behavior has been reviewed (Swanson, 2000). The BSTdm innervates both regions.

Visceromotor-related—This category can be further divided into those related to the neuroendocrine system, brainstem preautonomic cell groups, cerebral nuclei (basal ganglia) associated with visceromotor responses, and the hypothalamic visceromotor pattern generator network.

<u>**Direct projections to neuroendocrine motoneuron pools:**</u> The BSTdm sends massive direct inputs to regions containing either magnocellular or parvicellular neuroendocrine motoneuron pools (for reviews see Swanson, 1986, 1987; Markakis and Swanson, 1997; Thompson and Swanson, 2003). The densest BSTdm projections to the paraventricular nucleus magnocellular division are to regions where oxytocinergic neuronal cell bodies predominate: the anterior part, medial zone of the posterior part, and circumference of the posterior part's lateral zone. In contrast, the BSTdm projections to the supraoptic nucleus are found caudally and ventrally, where vasopressinergic neuronal cell bodies predominate—as well as rostrally and dorsally where oxytocinergic cell bodies predominate. The BSTdm also densely innervates several clusters of magnocellular neurons forming part of the accessory supraoptic nucleus, where complex mixtures of oxytocinergic and vasopressinergic neurons may be found (Peterson, 1966; Duan and Ju, 1998; Khan et al., 1999).

The BSTdm also projects massively to regions containing the motoneuron pools for several classes of parvicellular neurosecretory neurons, although ultrastructural data is needed to establish which cell types are actually innervated directly by BSTdm axon terminals. From rostral to caudal, these cell groups include those synthesizing gonadotropin-releasing hormone (in and around the rostral end of the medial preoptic region), somatostatin (centered in the anterior periventricular nucleus and periventricular part of the paraventricular nucleus), thyrotropin-releasing hormone (centered in medial regions of the dorsal medial parvicellular part of the paraventricular nucleus), and corticotropin-releasing hormone (centered in lateral regions of the dorsal medial parvicellular part of the paraventricular nucleus). In contrast, regions containing pools of growth hormone-releasing hormone and dopamine (inhibiting prolactin release)—that is, the arcuate and posterior periventricular nuclei—receive sparse BSTdm inputs at best. Earlier anterograde and retrograde tracing experiments established the existence of projections from the BST to the region of the paraventricular, supraoptic, and periventricular nuclei (Sawchenko and Swanson, 1983; Risold et al., 1997; Spencer et al., 2005).

Projections to brainstem preautonomic cell groups: Several hypothalamic preautonomic cell groups receive dense BSTdm inputs. The clearest example is the dorsal parvicellular part of the paraventricular nucleus, where most if not all neurons project to the spinal cord (Sawchenko and Swanson, 1981)—to preganglionic cell groups and the marginal zone throughout the length of the cord (see Swanson and McKellar, 1979). A dense BSTdm input to this part of the paraventricular nucleus suggests a direct influence on preautonomic projections to sympathetic and parasympathetic preganglionic neurons in the spinal cord. This is strengthened by evidence that pseudorabies virus injections in the stellate ganglion, adrenal gland, and pancreas retrogradely label upper order neurons in the region of the BSTdm (Smith et al., 1998; Westerhaus and Loewy, 1999).

Second, the BSTdm projects very densely to two parts of the paraventricular nucleus that project to both the spinal cord and dorsal vagal complex (including the dorsal motor nucleus): the lateral and ventral medial parvicellular parts (see Saper et al., 1976; Swanson and Kuypers, 1980b). Fluorogold injections centered in the former retrogradely label many neurons in the BSTdm, and in the BST magnocellular, ventral, and fusiform nuclei (Lori Gorton and Alan G. Watts, personal communication).

Third, the BSTdm projects to several hypothalamic regions that contain preautonomic neurons intermixed extensively with other cell types—making an input specifically to preautonomic neurons possible but considerably more uncertain. They include especially the retrochiasmatic area and posterior hypothalamic nucleus (see Saper et al., 1976; Swanson and Kuypers, 1980a).

Fourth, the BSTdm sends a massive, very circumscribed projection to Barrington's nucleus in the pontine central gray, hints of which are found in earlier axonal transport tracing experiments (Moga et al., 1990; Valentino et al., 1994). Well established projections from Barrington's nucleus to lumbosacral regions of the spinal cord that innervate parasympathetic components of the pelvic nerves to the urinary bladder, distal colon, and genitals (Satoh et al., 1978; Loewy et al., 1979; Pavcovich et al., 1998; Cano et al., 2000; Valentino et al., 2000; for reviews see Monnier, 1968; Appenzeller, 1990; De Groat and Steers, 1990; Blok and Holstege, 1996) are critical for controlling micturition, defecation, and penile erection (see Dong and Swanson, 2005a). Interestingly, the retrochiasmatic area and posterior hypothalamic area (which receive an input from the BSTdm) also project to Barrington's nucleus (Allen and Cechetto, 1992; Valentino et al., 1994; Vertes and Crane, 1996).

And fifth, BSTdm projections to the periaqueductal gray are densest in the ventrolateral division. Stimulation in this region produces a variety of autonomic responses, including cardiovascular related (see Carrive and Bandler, 1991; Behbehani, 1995; Saper, 2002), at least partly via projections to the caudal raphé nuclei and adjacent gigantocellular reticular nucleus, and the ventrolateral medulla (see Carrive and Bandler, 1991; Van Bockstaele et al., 1991; Cameron et al., 1995; Farkas et al., 1997, 1998). All of these regions receive an input from the BSTdm. Retrograde tracing experiments support the existence of a projection from a broad region including the BSTdm to the ventrolateral periaqueductal gray (Gray and Magnuson, 1992), the raphé pallidus and adjacent gigantocellular reticular nucleus (Hermann et al., 1997), raphé pallidus (Hermann et al., 1997; Nogueira et al., 2000), and ventrolateral medulla (Hardy, 2001).

Projections to cerebral hemisphere nuclei involved in visceromotor responses: The central amygdalar nucleus, and several components of the BST anterolateral group that are substantially innervated by the BSTdm (including the rhomboid and fusiform nuclei, and caudal anterolateral area), may be regarded as part of a striatopallidal differentiation

involved in regulating autonomic and/or neuroendocrine responses, based on developmental, connectional, fast neurotransmitter utilization, and functional evidence (Swanson and Petrovich, 1998; Swanson, 2000, 2003; Dong et al., 2001a,b; Dong and Swanson, 2003, 2004a). Specifically, the medial part of the central amygdalar nucleus, which receives a dense BSTdm input, and the BST rhomboid nucleus send dense projections to the dorsal motor nucleus of the vagus nerve (Hopkins and Holstege, 1978; Holstege et al., 1985; Liubashina et al., 2000; Dong and Swanson, 2003), whereas the BST fusiform nucleus sends dense projections to the lateral parvicellular and forniceal parts of paraventricular nucleus (preautonomic) and medial dorsal parvicellular part of the paraventricular nucleus where the corticotropin-releasing hormone neuroendocrine motoneuron pool is centered (Dong et al., 2001b). In addition, the medial and capsular parts of the central amygdalar nucleus, and specific parts of the BST anterolateral group send dense projections to the dorsal region and parasubthalamic nucleus of the lateral hypothalamic area, ventrolateral periaqueductal gray, parabrachial nucleus, and nucleus of the solitary tract (Hopkins and Holstege, 1978; Holstege et al., 1985; Liubashina et al., 2000; Dong et al., 2001a; Dong and Swanson, 2003a,b)—all parts of the central autonomic control system. In addition, the central amygdalar nucleus and BST anterolateral region have been implicated in drinking behavior and sodium appetite (see Johnson and Thunhorst, 1997; Watts, 2000).

Finally, the BSTam, which receives a dense input from the BSTdm, sends massive projections to the region of hypothalamic neuroendocrine motoneuron pools (Dong and Swanson, 2005a). Two other cerebral nuclei that receive modest input from the BSTdm, the lateral septal and anterodorsal medial amygdalar nuclei, are also important for controlling neuroendocrine and autonomic responses associated with motivated behavior (Canteras et al., 1995; Risold and Swanson, 1997b).

Projections to hypothalamic visceromotor pattern generator: The BSTdm projects to all six components of the recently identified hypothalamic visceromotor pattern generator (HVPG) network that is in a position to coordinate complex autonomic and neuroendocrine responses (Thompson and Swanson, 2003). These cell groups include the dorsomedial hypothalamic and median preoptic nuclei (which are the most densely innervated by the BSTdm), the parastrial and the anteroventral and anterodorsal preoptic nuclei (which receive substantial inputs from the BSTdm), and the anteroventral periventricular nucleus (which receives only a sparse input). All six HVPG nuclei are massively interconnected themselves, and each HVPG nucleus generates a pattern of terminal fields that differentially targets a unique set of hypothalamic neuroendocrine motor neuron pools and of preautonomic parts of the paraventricular nucleus. All five HVPG nuclei that are substantially innervated by the BSTdm send only sparse inputs to the region of growth hormone-releasing hormone and dopamine neuroendocrine motor neuron pools in the arcuate nucleus (Thompson and Swanson, 2003), which also receives only a sparse input from the BSTdm itself. However, the anteroventral periventricular nucleus, which receives a sparse input from the BSTdm, sends the densest HVPG input to the growth hormone-releasing hormone and dopamine neuroendocrine motor neuron pool regions of the arcuate nucleus (Thompson and Swanson, 2003).

Projections to rostral behavior control column—Along with its well known autonomic projections (mentioned above), the descending division of the paraventricular hypothalamic nucleus plays a critical role in the expression of drinking and eating behaviors (see Swanson, 2000; Watts, 2001) and for this reason has been included in the rostral behavior control column (Swanson, 2000; Thompson and Swanson, 2003). The BSTdm also provides substantial inputs to the lateral part of the medial preoptic nucleus, a component of the rostral behavioral control column involved in the expression of masculine sexual behavior, and to the anterior hypothalamic nucleus, a component involved in the expression

of defensive behavior. A few retrogradely labeled neurons were observed in the vicinity of the BSTdm after retrograde tracer injections in the medial preoptic nucleus (Simerly and Swanson, 1986).

Projections to caudal behavior control column—The most obvious component here is the ventral tegmental area, which—along with the interconnected nucleus accumbens and substantia innominata—has been implicated in the control of locomotor behavior and reward expectation (see Swanson et al., 1984; Mogenson et al., 1985; Wilson et al., 1995; Mogenson, 1987; Groenewegen et al., 1996; Ikemoto and Panksepp, 1999; Kelley, 1999; Parkinson et al., 1999; Tzschentke and Schmidt, 2000; Reynolds and Berridge, 2002; Wise, 2002). The BSTdm innervates all three regions.

Projections to orofacial motor control region—This category includes a substantial input to the retrorubral area of the midbrain reticular nucleus, an area that has been implicated in modulating orofacial behaviors (reviewed in Dong and Swanson, 2003).

Projections to thalamocortical loops—The present results indicate that caudal regions of the paraventricular thalamic nucleus receive a major input from the BSTdm, and that the latter also provides substantial inputs to caudal regions of the central medial nucleus, the intermediodorsal nucleus, the medial part of the mediodorsal nucleus, and the nucleus reuniens. Projections from the general region of the BSTdm to the mediodorsal and paraventricular nuclei have been retrogradely labeled (Cornwall and Phillipson, 1988; Groenewegen, 1988). Together these midline/medial/intralaminar thalamic nuclei project to a rather extensive band of cortex that includes the anterior cingulate area, prelimbic and infralimbic areas of the prefrontal region, agranular insular area, perirhinal area of the ventral temporal region, and entorhinal area and ventral subiculum of the hippocampal formation (see Groenewegen, 1988; Berendse and Groenewegen, 1991; Risold et al., 1997). In contrast to the BST anterolateral group, the BSTdm projects substantially to the lateral habenula of the epithalamus, especially to its caudal end.

Projections to behavioral state control nuclei—A number of brain structures innervated by the BSTdm play important roles in controlling behavioral state—circadian rhythms and the sleep/wake cycle, and arousal level in the waking state. First, the hypothalamic subparaventricular zone receives a dense BSTdm input. It is the major target of neural projections from the suprachiasmatic nucleus (which also receives a minor input from the BSTdm), and it projects to the same general regions as the suprachiasmatic nucleus (Watts and Swanson, 1987; Watts et al., 1987; Moga and Moore, 1997; Krout et al., 2002). The role of the suprachiasmatic nucleus and subparaventricular zone in generating and distributing circadian information to the rest of the brain is well known (see Lu et al., 2001; Moore and Danchenko, 2002).

Second, a number of hypothalamic regions thought to be involved in regulating the sleep/ wake cycle and behavioral arousal are innervated by the BSTdm. They include a) the ventrolateral preoptic nucleus, with GABA/galaninergic neurons that are active during sleep (Sherin et al., 1996, 1998; Gaus et al., 2002; Lu et al., 2002); b) the ventral tuberomammillary nucleus, with GABA/histaminergic neurons that promote wakefulness (see Köhler et al., 1985; Scammell et al., 2000); c) the dorsal region of the lateral hypothalamic area, with its separate populations of melanin-concentrating hormone containing and hypocretin/orexin-containing neurons modulating the sleep-wake cycle and arousal in ways that remain to be fully characterized (see Broberger et al., 1998; Elias et al., 1998; Chemelli et al., 1999; Saper et al., 2001; Willie et al., 2001; Taheri et al., 2002); and d) the supramammillary and posterior hypothalamic nuclei, which play an important role in modulating hippocampal theta rhythm, which in turn is present during exploratory behavior

and the rapid eye movement stage of sleep (see Vertes and Kocsis, 1997). The general region of the lateral hypothalamic area mentioned in c) also appears to play an important role in the expression of eating and drinking behaviors (e.g., Yamamoto et al., 1989; Elias et al., 1999; Khan et al., 1999; Stratford and Kelley, 1999; Watts et al., 1999; Petrovich et al., 2002).

Third, the BSTdm projects to a number of brainstem raphé components that have various combinations of serotonergic and non-serotonergic neurons: the interfascicular, rostral linear, central linear, dorsal raphé, raphé magnus, raphé pallidus, and raphé obscurus. Retrograde tracer studies reported projections from the general region containing the BSTdm to the raphé magnus and adjacent gigantocellular reticular nucleus (Hermann et al., 1997), and to raphé pallidus (Hermann et al., 1997; Nogueira et al., 2000).

And fourth, the caudal lateral habenula receives a substantial input from the BSTdm. It projects massively to a highly interconnected trio of midline nuclei near the midbrain-hindbrain junction: the interpeduncular nucleus, superior central nucleus (median raphé), and nucleus incertus—which are in a position to modulate behavioral state during motivated behavior (see Herkenham and Nauta, 1979; Motohashi et al., 1986; Araki et al., 1988; Lee and Huang, 1988; Goto et al., 2001). BST inputs to the lateral habenula were reported in the retrograde tracer study of Li and colleagues (1993).

Functional implications: neural inputs

Fragmentary structural evidence suggests that the BSTdm receives direct neural inputs from the cerebral cortex and cerebral nuclei (striatopallidum), brainstem viscerosensory nuclei, and brainstem regions related to behavioral state control (Fig. 11).

Cerebral inputs—PHAL experiments indicate that the following interconnected cortical regions project directly in rats to the region of the BSTdm: the posterior cortical nucleus, piriform-amygdalar area, postpiriform transition area, and basomedial nuclei of the amygdalar region (dealing predominantly with main and accessory olfactory inputs); the ventral subiculum and lateral entorhinal area (components of the hippocampal trisynaptic circuit); and the infralimbic prefrontal area (olfactory and visceral sensorimotor) (see Brittain, 1988; McDonald et al., 1999; Dong et al., 2001a).

The BSTdm receives a major input from the anterodorsal part of the medial amygdalar nucleus, and a minor input from the posteroventral part (Canteras et al., 1995; Dong et al., 2001a)—which may be regarded as caudal differentiations of the striatum (Swanson and Petrovich, 1998) that receive inputs from the three cortical regions just mentioned, as well as the ventral agranular insular area (olfactory, visceral sensorimotor, and other polymodal sensory), and the accessory olfactory bulb, which clearly predominates (Scalia and Winans, 1975). The role of the medial nucleus in the transmission of pheromonal information, and the expression of reproductive and defensive behaviors, has been reviewed recently (Dong and Swanson 2004b). The medial nucleus has also been implicated in the expression of sodium appetite (Johnson et al., 1999). This is interesting in light of its projections to the BSTdm, which in turn projects to the subfornical organ and region of the lamina terminalis (Fig. 11).

The BSTdm is also innervated moderately by ventral regions of the capsular part of the central amygdalar nucleus, and lightly by its medial part (Dong et al., 2001a). The central nucleus may be regarded as another caudal differentiation of the striatum, specialized for influencing autonomic responses (Swanson and Petrovich, 1998). In addition, the BSTdm is innervated by the BST rhomboid nucleus (Dong and Swanson, 2003) and caudal substantia

innominata (Grove, 1988a), both of which receive inputs from the central amygdalar nucleus (Grove, 1988b; Sun and Cassell, 1993; Dong and Swanson, 2003).

Brainstem sensory inputs—It seems likely that the BSTdm receives direct inputs from the nucleus of the solitary tract (Ricardo and Ko, 1978) and central part of the lateral division of the parabrachial nucleus (Alden et al., 1994). The latter receives inputs from the medial part of the nucleus of the solitary tract, which processes general visceral sensory information (Herbert et al., 1990). Recall that the same part of the parabrachial nucleus receives an input from the BSTdm.

The subfornical organ, which receives a BSTdm input, also sends a projection to the vicinity of the BSTdm, and it may use angiotensin II as a neurotransmitter (Swanson and Lind, 1986). Anteroventral territories of the BST including the BSTdm contain abundant angiotensin II-immunoreactive fibers (Lind et al., 1985) and very high levels of angiotensin II receptors (Grove et al., 1991; Denton et al., 1996) that could be activated by relatively low blood levels of angiotensin II (McKinley et al., 1998). The BSTdm also projects to the region of the vascular organ of the lamina terminalis/median preoptic nucleus, which projects back massively to the BSTdm (Thompson and Swanson, 2003). Sunn et al. (2003) showed that neurons in the subfornical organ and region of the vascular organ of the lamina terminalis that project to the BST express fos protein in response to elevated circulating levels of angiotensin II.

In summary, humoral and neural inputs associated with water and electrolyte balance, energy balance, and other classes of viscerosensation converge on the BSTdm, and the general area of the BST containing the BSTdm has been implicated in angiotensin II-induced drinking behavior, and in salt appetite.

Inputs related to behavioral state—Anteroventral regions of the BST including the BSTdm appear to receive inputs from: a) lateral regions of the lateral hypothalamic area (Allen and Cechetto, 1993), b) the medial and lateral parts of the supramammillary nucleus (Vertes, 1992), c) histaminergic neurons of the tuberomammillary nucleus (Inagaki et al., 1988), d) dopaminergic neurons of the ventral tegmental and adjacent retrorubral areas (Deutch et al., 1988; Hasue and Shammah-Lagnado, 2002), e) serotonergic neurons of the raphé nuclei (Vertes, 1991), and noradrenergic neurons of the locus ceruleus and nucleus of the solitary tract (Swanson and Hartman, 1975; Ricardo and Koh, 1978; Jones and Yang, 1985; Risold and Swanson, 1997a).

Overview

The projections of the BST rhomboid nucleus, reported previously (Dong & Swanson, 2003) suggest that it plays an important role in cerebral hemisphere control of ingestive behavior, and more specifically that it forms part of a cortico-striatopallidal system involved preferentially, though not exclusively, in the voluntary regulation of eating behavior and associated homeostatic responses. The evidence presented and reviewed here suggests that the BSTdm also plays a critical role in cerebral hemisphere control of ingestive behavior, but in contrast forms part of a cortico-striatopallidal system involved preferentially, though not exclusively, in the voluntary regulation of drinking behavior. However, it is also important to point out that the BSTdm generates very extensive direct projections to many parts of the hypothalamic neuroendocrine system, and to the hypothalamic visceromotor pattern generator network that appears to control its output. In fact, the BSTdm has the densest inputs directly to the neuroendocrine system of any cerebral hemisphere component examined to date.

Acknowledgments

ABBREVIATIONS

AAA	anterior amygdalar area
ac	anterior commissure
ACAd	anterior cingulate area, dorsal part
ACB	nucleus accumbens
aco	anterior commissure, olfactory limb
act	anterior commissure, temporal limb
ACVII	accessory facial nucleus
AD	anterodorsal nucleus
ADP	anterodorsal preoptic nucleus
AHA	anterior hypothalamic area
AHN	anterior hypothalamic nucleus
AHNa	anterior hypothalamic nucleus, anterior part
AHNc	anterior hypothalamic nucleus, central part
AHNd	anterior hypothalamic nucleus, dorsal part
AHNp	anterior hypothalamic nucleus, posterior part
AI	agranular insular area
AId	agranular insular area, dorsal part
AIv	agranular insular area, ventral part
AMBd	nucleus ambiguus, dorsal part
AMBv	nucleus ambiguus, ventral part
amc	amygdalar capsule
AMd	anteromedial nucleus thalamus, dorsal part
AMv	anteromedial nucleus thalamus, ventral part
AOB	accessory olfactory bulb
AQ	cerebral aqueduct
ARH	arcuate nucleus hypothalamus
ASO	accessory supraoptic group
AV	anteroventral nucleus thalamus
AVP	anteroventral preoptic nucleus
AVPV	anteroventral periventricular nucleus
B	Barrington's nucleus
BA	bed nucleus accessory olfactory tract
BAC	bed nucleus anterior commissure

bic	brachium inferior colliculus
BLAa	basolateral nucleus amygdala, anterior part
BLAp	basolateral nucleus amygdala, posterior part
BMAa	basomedial nucleus amygdala, anterior part
BMAp	basomedial nucleus amygdala, posterior part
bp	bouton of passage
bsc	brachium superior colliculus
BST	bed nuclei of the stria terminalis
BSTal	bed nuclei of the stria terminalis, anterior division, anterolateral area
BSTalg	bed nuclei of the stria terminalis, anterior division, anterolateral group
BSTam	bed nuclei of the stria terminalis, anterior division, anteromedial area
BSTamg	bed nuclei of the stria terminalis, anterior division, anteromedial group
BSTd	bed nuclei of the stria terminalis, posterior division, dorsal nucleus
BSTdm	bed nuclei of the stria terminalis, anterior division, dorsomedial nucleus
BSTfu	bed nuclei of the stria terminalis, anterior division, fusiform nucleus
BSTif	bed nuclei of the stria terminalis, posterior division, interfascicular nucleus
BSTju	bed nuclei of the stria terminalis, anterior division, juxtacapsular nucleus
BSTmg	bed nuclei of the stria terminalis, anterior division, magnocellular nucleus
BSTov	bed nuclei of the stria terminalis, anterior division, oval nucleus
BSTp	bed nuclei of the stria terminalis, posterior division
BSTpr	bed nuclei of the stria terminalis, posterior division, principal nucleus
BSTrh	bed nuclei of the stria terminalis, anterior division, rhomboid nucleus
BSTse	bed nuclei of the stria terminalis, posterior division, stria extension
BSTsz	bed nuclei of the stria terminalis, posterior division, cell-sparse zone
BSTtr	bed nuclei of the stria terminalis, posterior division, transverse nucleus
BSTv	bed nuclei of the stria terminalis, anterior division, ventral nucleus
CA1	field CA1, Ammon's horn
CA3	field CA3, Ammon's horn
CEA	central nucleus amygdala
CEAc	central nucleus amygdala, capsular part
CEAl	central nucleus amygdala, lateral part
CEAm	central nucleus amygdala, medial part
CLA	claustrum
CLI	central linear nucleus raphé
CM	central medial nucleus thalamus
COAa1,2	cortical nucleus amygdala, anterior part, layers 1, 2

COApl	cortical nucleus amygdala, posterior part, lateral zone
COApm	cortical nucleus amygdala, posterior part, medial zone
COM	commissural nucleus, periaqueductal gray
CP	caudoputamen
cpd	cerebral peduncle
CRH	corticotropin releasing hormone
csc	superior colliculus commissure
CSl	superior central nucleus raphé, lateral part
CSm	superior central nucleus raphé, medial part
CUN	cuneiform nucleus
DMH	dorsomedial nucleus hypothalamus
DMHa	dorsomedial nucleus hypothalamus, anterior part
DMHp	dorsomedial nucleus hypothalamus, posterior part
DMHv	dorsomedial nucleus hypothalamus, ventral part
DMX	dorsal motor nucleus vagus nerve
DR	dorsal nucleus raphé
dscp	decussation superior cerebellar peduncle
dtd	dorsal tegmental decussation
DTN	dorsal tegmental nucleus
ec	external capsule
em	external medullary lamina
EPd	endopiriform nucleus, dorsal part
EPv	endopiriform nucleus, ventral part
EW	Edinger-Westphal nucleus
FF	fields of Forel
fi	fimbria
fr	fasciculus retroflexus
FS	fundus of the striatum
fx	columns of the fornix
GnRH	gonadotropin releasing hormone
GPe	globus pallidus, external segment
GRN	gigantocellular reticular nucleus
GU	gustatory area
HF	hippocampal formation
I	internuclear area
IA	intercalated nuclei amygdala

IAD	interanterodorsal nucleus thalamus
IAM	interanteromedial nucleus thalamus
ICe	inferior colliculus, external nucleus
IF	interfascicular nucleus raphé
III	oculomotor nucleus
ILA	infralimbic cortical area
im	internal medullary lamina thalamus
IMD	intermediodorsal nucleus thalamus
INC	interstitial nucleus of Cajal
int	internal capsule
IOma	inferior olivary complex, medial accessory olive
IPN	interpeduncular nucleus
IPNc	interpeduncular nucleus, central subnucleus
isl	islands of Calleja
islm	major islands of Calleja
ISN	inferior salivatory nucleus
IVn	trochlear nerve
KF	Kölliker-Fuse subnucleus (of PB)
LA	lateral amygdalar nucleus
LC	locus ceruleus
LDT	laterodorsal tegmental nucleus
LGvm	lateral geniculate complex, ventral division, medial zone
LH	lateral habenula
LHA	lateral hypothalamic area
LHAad	lateral hypothalamic area, anterior region, dorsal zone
LHAai	lateral hypothalamic area, anterior region, intermediate zone
LHAav	lateral hypothalamic area, anterior region, ventral zone
LHAd	lateral hypothalamic area, dorsal region
LHAjd	lateral hypothalamic area, juxtadorsomedial region
LHAjp	lateral hypothalamic area, juxtaparaventricular region
LHAjvd	lateral hypothalamic area, juxtaventromedial region, dorsal zone
LHAjvv	lateral hypothalamic area, juxtaventromedial region, ventral zone
LHAm	lateral hypothalamic area, magnocellular nucleus
LHAp	lateral hypothalamic area, posterior region
LHApc	lateral hypothalamic area, parvicellular region
LHAs	lateral hypothalamic area, suprafornical region

LHAsfa	lateral hypothalamic area, subfornical region, anterior zone
LHAsfp	lateral hypothalamic area, subfornical region, posterior zone
LHAsfpm	lateral hypothalamic area, subfornical region, premammillary zone
LHAvl	lateral hypothalamic area, ventral region, lateral zone
LHAvm	lateral hypothalamic area, ventral region, medial zone
LM	lateral mammillary nucleus
lot	lateral olfactory tract
LP	lateral posterior nucleus
LPO	lateral preoptic area
LS	lateral septal nucleus
LSc	lateral septal nucleus, caudal part
LSc.d.r	lateral septal nucleus, caudal part, dorsal zone, rostral region
LSc.v.i	lateral septal nucleus, caudal part, ventral zone, intermediate region
LSc.v.l.d/v	lateral septal nucleus, caudal part, ventral zone, lateral region, dorsal/ventral domains
LSc.v.m.d/v	lateral septal nucleus, caudal part, ventral zone, medial region, dorsal/ventral domains
LSr	lateral septal nucleus, rostral part
LSr.dl.l.d/v	lateral septal nucleus, rostral part, dorsolateral zone, lateral region, dorsal/ventral domains
LSr.dl.m.d/v	lateral septal nucleus, rostral part, dorsolateral zone, medial region, dorsal/ventral domains
LSr.m	lateral septal nucleus, rostral part, medial zone
LSr.m.d	lateral septal nucleus, rostral part, medial zone, ventral region, caudal domain
LSr.m.v.c/d/r	lateral septal nucleus, rostral part, medial zone, ventral region, caudal/dorsal/rostral domains
LSr.vl.d.l/m	lateral septal nucleus, rostral part ventrolateral zone, dorsal region, lateral/medial domains
LSr.vl.v	lateral septal nucleus, rostral part, ventrolateral zone, ventral region
LSv	lateral septal nucleus, ventral part
LTN	lateral tegmental nucleus
MA	magnocellular preoptic nucleus
MARN	magnocellular reticular nucleus
mct	medial corticohypothalamic tract
MDc	mediodorsal nucleus thalamus, central part
MDm	mediodorsal nucleus thalamus, medial part

MDRNd	medullary reticular nucleus, dorsal part
MDRNv	medullary reticular nucleus, ventral part
ME	median eminence
MEAad	medial nucleus amygdala, anterodorsal part
MEAav	medial nucleus amygdala, anteroventral part
MEApd-a,b,c	medial nucleus amygdala, posterodorsal part, sublayers a-c
MEApv	medial nucleus amygdala, posteroventral part
MEPO	median preoptic nucleus
MEV	midbrain nucleus of the trigeminal
MH	medial habenula
ml	medial lemniscus
mlf	medial longitudinal fascicle
MM	medial mammillary nucleus
MOB	main olfactory bulb
MOC	main olfactory cortex
MoV	motor root of the trigeminal
mp	mammillary peduncle
MPN	medial preoptic nucleus
MPNc	medial preoptic nucleus, central part
MPNl	medial preoptic nucleus, lateral part
MPNm	medial preoptic nucleus, medial part
MPO	medial preoptic area
MRN	midbrain reticular nucleus
MRNm	midbrain reticular nucleus, magnocellular part
MRNp	midbrain reticular nucleus, parvicellular part
MS	medial septal nucleus
MT	medial terminal nucleus accessory optic tract
mtg	mammillotegmental tract
mtt	mammillothalamic tract
mtV	midbrain tract of the trigeminal nerve
NB	nucleus brachium inferior colliculus
NC	nucleus circularis
ND	nucleus of Darkschewitsch
NDB	nucleus of the diagonal band
NId	nucleus incertus, dorsal part

NLL	NLL nucleus of the lateral lemniscus
NLOT	nucleus of the lateral olfactory tract
NLOT1	nucleus of the lateral olfactory tract, molecular layer
NLOT2	nucleus of the lateral olfactory tract, pyramidal layer
NLOT3	nucleus of the lateral olfactory tract, dorsal cap
NPC	nucleus of the posterior commissure
NTSl	nucleus of the solitary tract, lateral part
NTSm	nucleus of the solitary tract, medial part
och	optic chiasm
opt	optic tract
ORBm	orbital area, medial part
ORBv2,3	orbital area, ventral part, layers 2, 3
OT	olfactory tubercle
OT1	olfactory tubercle, molecular layer
OT2	olfactory tubercle, pyramidal layer
OT3	olfactory tubercle, polymorph layer
OV	vascular organ lamina terminalis
OXY	oxytocin
PA	posterior nucleus amygdala
PAG	periaqueductal gray
PAGd	periaqueductal gray, dorsal division
PAGdl	periaqueductal gray, dorsolateral division
PAGm	periaqueductal gray, medial division
PAGrl	periaqueductal gray, rostrolateral division
PAGrm	periaqueductal gray, rostromedial division
PAGvl	periaqueductal gray, ventrolateral division
PB	parabrachial nucleus
PBlc	parabrachial nucleus, central lateral part
PBle	parabrachial nucleus, external lateral part
PBls	parabrachial nucleus, superior lateral part
PBlv	parabrachial nucleus, ventral lateral part
PBme	parabrachial nucleus, external medial part
PBmm	parabrachial nucleus, medial medial part
PBmv	parabrachial nucleus, ventral medial part
pc	posterior commissure
PCG	pontine central gray

PD	posterodorsal preoptic nucleus
PF	parafascicular nucleus
PGRN	paragigantocellular reticular nucleus
PGRNl	paragigantocellular reticular nucleus, lateral part
PH	posterior hypothalamic nucleus
PIR	piriform area
PIR1	piriform area, molecular layer
PIR2	piriform area, pyramidal layer
PIR3	piriform area, polymorph layer
PL	prelimbic cortical area
pm	principal mammillary tract
PMd	dorsal premammillary nucleus
PMv	ventral premammillary nucleus
POR	periolivary region
PP	peripeduncular nucleus
PPN	pedunculopontine nucleus
PPYd	parapyramidal nucleus, deep part
PR	perireuniens nucleus
PRC	precommissural nucleus, periaqueductal gray
PRNc	pontine reticular nucleus, caudal part
PRNr	pontine reticular nucleus, rostral part
PS	parastrial nucleus
PSCH	suprachiasmatic preoptic nucleus
PST	preparasubthalamic nucleus
PSTN	parasubthalamic nucleus of the lateral hypothalamic area
PT	paratenial nucleus
PVa	anterior periventricular nucleus hypothalamus
PVH	paraventricular nucleus hypothalamus
PVHam	paraventricular nucleus hypothalamus, anterior magnocellular part
PVHap	paraventricular nucleus hypothalamus, anterior parvicellular part
PVHd	paraventricular nucleus hypothalamus, descending division
PVHdp	paraventricular nucleus hypothalamus, dorsal parvicellular part
PVHf	paraventricular nucleus hypothalamus, forniceal part
PVHlp	paraventricular nucleus hypothalamus, lateral parvicellular part
PVHmpd	paraventricular nucleus hypothalamus, medial parvicellular part, dorsal zone

PVHmpv	paraventricular nucleus hypothalamus, medial parvicellular part, ventral zone
PVHne	paraventricular nucleus hypothalamus, neuroendocrine division
PVHpml	paraventricular nucleus hypothalamus, posterior magnocellular part, lateral zone
PVHpmm	paraventricular nucleus hypothalamus, posterior magnocellular part, medial zone
PVHpv	paraventricular nucleus hypothalamus, periventricular part
PVi	intermediate periventricular nucleus hypothalamus
PVp	posterior periventricular nucleus hypothalamus
PVpo	preoptic periventricular nucleus
PVT	paraventricular nucleus thalamus
py	pyramid
RCH	retrochiasmatic area
RE	nucleus reuniens
REa	nucleus reuniens, rostral division, anterior part
REcd	nucleus reuniens, caudal division, dorsal part
REcm	nucleus reuniens, caudal division, median part
REcp	nucleus reuniens, caudal division, posterior part
REd	nucleus reuniens, rostral division, dorsal part
REl	nucleus reuniens, rostral division, lateral part
REm	nucleus reuniens, rostral division, medial part
REv	nucleus reuniens, rostral division, ventral part
RH	rhomboid nucleus
RL	rostral linear nucleus raphé
RM	nucleus raphé magnus
RN	red nucleus
RO	nucleus raphé obscurus
RPA	nucleus raphé pallidus
RR	midbrain reticular nucleus, retrorubral area
RT	reticular nucleus thalamus
rust	rubrospinal tract
SBPV	subparaventricular zone hypothalamus
SC	superior colliculus
SCdg	superior colliculus, deep gray layer
SCdw	superior colliculus, deep white layer
SCH	suprachiasmatic nucleus

SCig-a,b,c	superior colliculus, intermediate gray layer, sublayers a-c
scp	superior cerebellar peduncle
sctv	ventral spinocerebellar tract
SF	septofimbrial nucleus
SFO	subfornical organ
SH	septohippocampal nucleus
SI	substantia innominata
SLC	subceruleus nucleus
SLD	sublaterodorsal nucleus
sm	stria medullaris
smd	supramammillary decussation
SNc	substantia nigra, compact part
SNr	substantia nigra, reticular part
SO	supraoptic nucleus
SOr	supraoptic nucleus, retrochiasmatic part
SPFm	subparafascicular nucleus thalamus, magnocellular part
SPFpl	subparafascicular nucleus thalamus, parvicellular part, lateral division
SPFpm	subparafascicular nucleus thalamus, parvicellular part, medial division
SPVI	spinal nucleus of the trigeminal, interpolar part
SS	somatostatin
SSN	superior salivatory nucleus
st	stria terminalis
STN	subthalamic nucleus
SUBv	subiculum, ventral part
SUM	supramammillary nucleus
SUMl	supramammillary nucleus, lateral part
SUMm	supramammillary nucleus, medial part
sup	supraoptic commissures
SUT	supratrigeminal nucleus
tb	terminal bouton
TMd	tuberomammillary nucleus, dorsal part
TMv	tuberomammillary nucleus, ventral part
TRH	thyrotropin releasing hormone
TRN	tegmental reticular nucleus
TRS	triangular nucleus septum

tsp	tectospinal pathway
TU	tuberal nucleus
TUi	tuberal nucleus, intermediate part
TUl	tuberal nucleus, lateral part
TUsv	tuberal nucleus, subventromedial part
TUte	tuberal nucleus, terete subnucleus
v	varicosity
V3	third ventricle
V3p	third ventricle, preoptic recess
V4	fourth ventricle
VAS	vasopressin
vhc	ventral hippocampal commissure
VII	facial nucleus
VIIn	facial nerve
VISC	visceral area
VL	lateral ventricle
VLP	ventrolateral preoptic nucleus
vlt	ventrolateral hypothalamic tract
VM	ventral medial nucleus thalamus
Vma	motor nucleus of the trigeminal, magnocellular part
VMHa	ventromedial nucleus hypothalamus, anterior part
VMHc	ventromedial nucleus hypothalamus, central part
VMHdm	ventromedial nucleus hypothalamus, dorsomedial part
VMHvl	ventromedial nucleus hypothalamus, ventrolateral part
Vpc	motor nucleus of the trigeminal, parvicellular part
VPMpc	ventral posteromedial nucleus thalamus, parvicellular part
VTA	ventral tegmental area
vtd	ventral tegmental decussation
VTN	ventral tegmental nucleus
XII	hypoglossal nucleus
ZI	zona incerta
ZIda	zona incerta, dopaminergic group
zl	zona limitans

LITERATURE CITED

Alden M, Besson JM, Bernard JF. Organization of the efferent projections from the pontine parabrachial area to the bed nucleus of the stria terminalis and neighboring regions: a PHA-L study in the rat. J Comp Neurol. 1994; 341:289–314. [PubMed: 7515078]

Allen GV, Cechetto DF. Functional and anatomical organization of cardiovascular pressor and depressor sites in the lateral hypothalamic area: I. Descending projections. J Comp Neurol. 1992; 315:313–332. [PubMed: 1740546]

Allen GV, Cechetto DF. Functional and anatomical organization of cardiovascular pressor and depressor sites in the lateral hypothalamic area. II. Ascending projections. J Comp Neurol. 1993; 330:421–438. [PubMed: 7682225]

Appenzeller, O. The autonomic nervous system: an introduction to basic and clinical concepts. Elsevier; Amsterdam: 1990. Neurogenic control and disorders of micturition; p. 443-489.

Araki M, McGeer PL, Kimura H. The efferent projections of the rat lateral habenular nucleus revealed by the PHA-L anterograde tracing method. Brain Res. 1988; 441:319–330. [PubMed: 2451982]

Behbehani MM. Functional characteristics of the midbrain periaqueductal gray. Prog Neurobiol. 1995; 46:575–605. [PubMed: 8545545]

Berendse HW, Groenewegen HJ. Restricted cortical termination fields of the midline and intralaminar thalamic nuclei in the rat. Neuroscience. 1991; 42:73–102. [PubMed: 1713657]

Bester H, Besson JM, Bernard JF. Organization of efferent projections from the parabrachial area to the hypothalamus: a Phaseolus vulgaris-leucoagglutinin study in the rat. J Comp Neurol. 1997; 383:245–281. [PubMed: 9205041]

Blok BF, Holstege G. The neuronal control of micturition and its relation to the emotional motor system. Prog Brain Res. 1996; 107:113–126. [PubMed: 8782516]

Bourque CW, Oliet SH. Osmoreceptors in the central nervous system. Ann Rev Physiol. 1997; 59:601–619. [PubMed: 9074779]

Brittain, DA. PhD thesis. Department of Neurosciences; University of California San Diego: 1988. The efferent connections of the infralimbic area in the rat.

Broberger C, De Lecea L, Sutcliffe JG, Hökfelt T. Hypocretin/orexin- and melanin-concentrating hormone-expressing cells form distinct populations in the rodent lateral hypothalamus: relationship to the neuropeptide Y and agouti gene-related protein systems. J Comp Neurol. 1998; 402:460–474. [PubMed: 9862321]

Cajal, SR. Histology of the nervous system in man and vertebrates. Swanson, N.; Swanson, LW., translators. Oxford University Press; New York: 1995.

Cameron AA, Khan IA, Westlund KN, Willis WD. The efferent projections of the periaqueductal gray in the rat: a Phaseolus vulgaris-leucoagglutinin study. II. Descending projections. J Comp Neurol. 1995; 351:585–601. [PubMed: 7721985]

Cano G, Card JP, Rinaman L, Sved AF. Connections of Barrington's nucleus to the sympathetic nervous system in rats. J Autonomic Nerv Syst. 2000; 79:117–128.

Canteras NS, Simerly RB, Swanson LW. Organization of projections from the medial nucleus of the amygdala: a PHAL study in the rat. J Comp Neurol. 1995; 360:213–245. [PubMed: 8522644]

Carrive P, Bandler R. Viscerotopic organization of neurons subserving hypotensive reactions within the midbrain periaqueductal grey: a correlative functional and anatomical study. Brain Res. 1991; 541:206–215. [PubMed: 2054638]

Chemelli RM, Willie JT, Sinton CM, Elmquist JK, Scammell T, Lee C, Richardson JA, Williams SC, Xiong Y, Kisanuki Y, Fitch TE, Nakazato M, Hammer RE, Saper CB, Yanagisawa M. Narcolepsy in orexin knockout mice: molecular genetics of sleep regulation. Cell. 1999; 98:437–451. [PubMed: 10481909]

Chou TC, Bjorkum AA, Gaus SE, Lu J, Scammell TE, Saper CB. Afferents to the ventrolateral preoptic nucleus. J Neurosci. 2002; 22:977–990. [PubMed: 11826126]

Conrad LC, Pfaff DW. Efferents from medial basal forebrain and hypothalamus in the rat. I. An autoradiographic study of the medial preoptic area. J Comp Neurol. 1976; 169:185–219. [PubMed: 61212]

Cornwall J, Phillipson OT. Afferent projections to the dorsal thalamus of the rat as shown by retrograde lectin transport. II. The midline nuclei. Brain Res Bull. 1988; 21:147–161. [PubMed: 3191403]

Cullinan WE, Herman JP, Watson SJ. Ventral subicular interaction with the hypothalamic nucleus: evidence for a relay in the bed nucleus of the stria terminalis. J Comp Neurol. 1993; 332:1–20. [PubMed: 7685778]

De Groat, WC.; Steers, WD. Autonomic regulation of the urinary bladder and sexual organs. In: Loewy, AD.; Spyer, KM., editors. Central regulation of autonomic functions. Oxford University Press; New York: 1990. p. 310-333.

Denton DA, McKinley MJ, Weisinger RS. Hypothalamic integration of body fluid regulation. Proc Natl Acad Sci USA. 1996; 93:7397–7404. [PubMed: 8693005]

Deutch AY, Goldstein M, Baldino F Jr. Roth RH. Telencephalic projections of the A8 dopamine cell group. Ann N Y Acad Sci. 1988; 537:27–50. [PubMed: 2462395]

Dierickx K. Immunocytochemical localization of the vertebrate cyclic nonapeptide neurohypophyseal hormones and neurophysins. Int Rev Cytol. 1980; 62:119–185. [PubMed: 6988359]

Dong H-W, Petrovich GD, Swanson LW. Organization of projections from the juxtacapsular nucleus of the BST: a PHAL study in the rat. Brain Res. 2000; 859:1–14. [PubMed: 10720609]

Dong H-W, Petrovich GD, Swanson LW. Topography of projections from amygdala to bed nuclei of the stria terminalis. Brain Res Rev. 2001a; 38:192–246. [PubMed: 11750933]

Dong H-W, Petrovich GD, Watts AG, Swanson LW. Basic organization of projections from the oval and fusiform nuclei of the bed nuclei of the stria terminalis in adult rat brain. J Comp Neurol. 2001b; 436:430–455. [PubMed: 11447588]

Dong H-W, Swanson LW. Projections from the rhomboid nucleus of the bed nuclei of the stria terminalis: implications for cerebral hemisphere regulation of ingestive behaviors. J Comp Neurol. 2003; 463:434–472. [PubMed: 12836178]

Dong H-W, Swanson LW. Organization of axonal projections from the anterolateral area of the bed nuclei of the stria terminalis. J Comp Neurol. 2004a; 468:277–298. [PubMed: 14648685]

Dong H-W, Swanson LW. Projections from bed nuclei of the stria terminalis, posterior division: implications for cerebral hemisphere regulation of defensive and reproductive behaviors. J Comp Neurol. 2004b; 471:396–433. [PubMed: 15022261]

Dong H-W, Swanson LW. Projections from the bed nuclei of the stria terminalis, magnocellular nucleus: implications for cerebral hemisphere regulation of micturition, defecation, and penile erection. J Comp Neurol. 2005a in press.

Dong H-W, Swanson LW. Projections from bed nuclei of the stria terminalis, anteromedial area: cerebral hemisphere integration of neuroendocrine, autonomic, and behavioral aspects of energy balance. J Comp Neurol. 2005b in press.

Duan X, Ju G. The organization of chemically characterized afferents to the perivascular neuronal groups of the hypothalamic magnocellular neurosecretory system in the rat. Brain Res Bull. 1998; 46:409–415. [PubMed: 9739002]

Elias CF, Aschkenasi C, Lee C, Kelly J, Ahima RS, Bjorbaek C, Flier JS, Saper CB, Elmquist JK. Leptin differentially regulates NPY and POMC neurons projecting to the lateral hypothalamic area. Neuron. 1999; 23:775–786. [PubMed: 10482243]

Elias CF, Saper CB, Maratos-Flier E, Tritos NA, Lee C, Kelly J, Tatro JB, Hoffman GE, Ollmann MM, Barsh GS, Sakurai T, Yanagisawa M, Elmquist JK. Chemically defined projections linking the mediobasal hypothalamus and the lateral hypothalamic area. J Comp Neurol. 1998; 402:442–459. [PubMed: 9862320]

Farkas E, Jansen AS, Loewy AD. Periaqueductal gray matter projection to vagal preganglionic neurons and the nucleus tractus solitarius. Brain Res. 1997; 764:257–261. [PubMed: 9295220]

Farkas E, Jansen AS, Loewy AD. Periaqueductal gray matter input to cardiac-related sympathetic premotor neurons. Brain Res. 1998; 792:179–192. [PubMed: 9593884]

Fitzsimons JT. Angiotensin, thirst, and sodium appetite. Physiol Rev. 1998; 78:583–686. [PubMed: 9674690]

Gaus SE, Strecker RE, Tate BA, Parker RA, Saper CB. Ventrolateral preoptic nucleus contains sleep-active, galaninergic neurons in multiple mammalian species. Neuroscience. 2002; 115:285–294. [PubMed: 12401341]

Gerfen CR, Sawchenko PE. An anterograde neuroanatomical tracing method that shows the detailed morphology of neurons, their axons and terminals: immunohistochemical localization of an axonally transported plant lectin, *Phaseolus vulgaris*-leucoagglutinin (PHA-L). Brain Res. 1984; 290:219–238. [PubMed: 6198041]

Gray TS, Magnuson DJ. Peptide immunoreactive neurons in the amygdala and the bed nucleus of the stria terminalis project to the midbrain central gray in the rat. Peptides. 1992; 13:451–460. [PubMed: 1381826]

Groenewegen HJ. Organization of the afferent connections of the mediodorsal thalamic nucleus in the rat, related to the mediodorsal-prefrontal topography. Neuroscience. 1988; 24:379–431. [PubMed: 2452377]

Groenewegen HJ, Wright CI, Beijer AV. The nucleus accumbens: gateway for limbic structures to reach the motor system? Prog Brain Res. 1996; 107:485–511. [PubMed: 8782538]

Grove EA. Efferent connections of the substantia innominata in the rat. J Comp Neurol. 1988a; 277:347–364. [PubMed: 2461973]

Grove EA. Neural associations of the substantia innominata in the rat: afferent connections. J Comp Neurol. 1988b; 277:315–346. [PubMed: 2461972]

Grove KL, Cook VI, Speth RC. Angiotensin II receptors in the ventral portion of the bed nucleus of the stria terminalis. Neuroendocrinology. 1991; 53:339–343. [PubMed: 2046868]

Hardy SG. Hypothalamic projections to cardiovascular centers of the medulla. Brain Res. 2001; 894:233–240. [PubMed: 11251196]

Hasue RH, Shammah-Lagnado SJ. Origin of the dopaminergic innervation of the central extended amygdala and accumbens shell: a combined retrograde tracing and immunohistochemical study in the rat. J Comp Neurol. 2002; 454:15–33. [PubMed: 12410615]

Herbert H, Moga MM, Saper CB. Connections of the parabrachial nucleus with the nucleus of the solitary tract and the medullary reticular formation in the rat. J Comp Neurol. 1990; 293:540–580. [PubMed: 1691748]

Herkenham M, Nauta WJ. Efferent connections of the habenular nuclei in the rat. J Comp Neurol. 1979; 187:19–47. [PubMed: 226566]

Hermann DM, Luppi PH, Peyron C, Hinckel P, Jouvet M. Afferent projections to the rat nuclei raphé magnus, raphe pallidus and reticularis gigantocellularis pars alpha demonstrated by iontophoretic application of choleratoxin (subunit b). J Chem Neuroanat. 1997; 13:1–21. [PubMed: 9271192]

Holstege G, Meiners L, Tan K. Projections of the bed nucleus of the stria terminalis to the mesencephalon, pons, and medulla oblongata in the cat. Exp Brain Res. 1985; 58:379–391. [PubMed: 3996501]

Hopkins DA, Holstege G. Amygdaloid projections to the mesencephalon, pons and medulla oblongata in the cat. Exp Brain Res. 1978; 32:529–547. [PubMed: 689127]

Ikemoto S, Panksepp J. The role of nucleus accumbens dopamine in motivated behavior: a unifying interpretation with special reference to reward-seeking. Brain Res Rev. 1999; 31:6–41. [PubMed: 10611493]

Johnson AK, de Olmos J, Pastuskovas CV, Zardetto-Smith AM, Vivas L. The extended amygdala and salt appetite. Ann N Y Acad Sci. 1999; 877:258–280. [PubMed: 10415654]

Johnson AK, Edwards GL. The neuroendocrinology of thirst: afferent signaling and mechanisms of central integration. Curr Top Neuroendocrinol. 1990; 10:149–190.

Jones BE, Yang TZ. The efferent projections from the reticular formation and the locus coeruleus studied by anterograde and retrograde axonal transport in the rat. J Comp Neurol. 1985; 242:56–92. [PubMed: 2416786]

Ju G, Swanson LW. Studies on the cellular architecture of the bed nuclei of the stria terminalis in the rat: I. Cytoarchitecture. J Comp Neurol. 1989; 280:587–602. [PubMed: 2708568]

Ju G, Swanson LW, Simerly RB. Studies on the cellular architecture of the bed nuclei of the stria terminalis in the rat: II. Chemoarchitecture. J Comp Neurol. 1989; 280:603–621. [PubMed: 2468695]

Kelley AE. Functional specificity of ventral striatal compartments in appetitive behaviors. Ann N Y Acad Sci. 1999; 877:71–90. [PubMed: 10415644]

Khan AM, Curras MC, Dao J, Jamal FA, Turkowski CA, Goel RK, Gillard ER, Wolfsohn SD, Stanley BG. Lateral hypothalamic NMDA receptor subunits NR2A and/or NR2B mediate eating: immunochemical/behavioral evidence. Am J Physiol. 1999; 276:R880–891. [PubMed: 10070151]

Köhler C, Swanson LW, Haglund L, Wu JY. The cytoarchitecture, histochemistry and projections of the tuberomammillary nucleus in the rat. Neuroscience. 1985; 16:85–110. [PubMed: 2423918]

Krout KE, Kawano J, Mettenleiter TC, Loewy AD. CNS inputs to the suprachiasmatic nucleus of the rat. Neuroscience. 2002; 110:73–92. [PubMed: 11882374]

Lee EH, Huang SL. Role of lateral habenula in the regulation of exploratory behavior and its relationship to stress in rats. Behav Brain Res. 1988; 30:265–271. [PubMed: 3178997]

Li YQ, Takada M, Shinonaga Y, Mizuno N. The sites of origin of dopaminergic afferent fibers to the lateral habenular nucleus in the rat. J Comp Neurol. 1993; 333:118–133. [PubMed: 8101849]

Lind RW, Swanson LW, Bruhn TO, Ganten D. The distribution of angiotensin II-immunoreactive cells and fibers in the paraventriculo-hypophysial system of the rat. Brain Res. 1985; 338:81–89. [PubMed: 3896394]

Lind RW, Swanson LW, Ganten D. Angiotensin II immunoreactivity in the neural afferents and efferents of the subfornical organ of the rat. Brain Res. 1984; 321:209–215. [PubMed: 6388733]

Liubashina O, Jolkkonen E, Pitkanen A. Projections from the central nucleus of the amygdala to the gastric related area of the dorsal vagal complex: a Phaseolus vulgaris-leucoagglutinin study in rat. Neurosci Lett. 2000; 291:85–88. [PubMed: 10978580]

Loewy AD, Saper CB, Baker RP. Descending projections from the pontine micturition center. Brain Res. 1979; 172:533–538. [PubMed: 476495]

Lu J, Bjorkum AA, Xu M, Gaus SE, Shiromani PJ, Saper CB. Selective activation of the extended ventrolateral preoptic nucleus during rapid eye movement sleep. J Neurosci. 2002; 22:4568–4576. [PubMed: 12040064]

Lu J, Zhang YH, Chou TC, Gaus SE, Elmquist JK, Shiromani P, Saper CB. Contrasting effects of ibotenate lesions of the paraventricular nucleus and subparaventricular zone on sleep-wake cycle and temperature regulation. J Neurosci. 2001; 21:4864–4874. [PubMed: 11425913]

Markakis EA, Swanson LW. Spatiotemporal patterns of secretomotor neuron generation in the parvicellular neuroendocrine system. Brain Res Rev. 1997; 24:255–291. [PubMed: 9385456]

McDonald, AJ. Cell types and intrinsic connections of the amygdala. In: Aggleton, JP., editor. The amygdala: neurobiological aspects of emotion, memory, and mental dysfunction. Wiley-Liss; New York: 1992. p. 67-99.

McDonald AJ, Shammah-Lagnado SJ, Shi C, Davis M. Cortical afferents to the extended amygdala. Ann N Y Acad Sci. 1999; 877:309–338. [PubMed: 10415657]

McKinley MJ, Allen AM, Burns P, Colvill LM, Oldfield BJ. Interaction of circulating hormones with the brain: the roles of the subfornical organ and the organum vasculosum of the lamina terminalis. Clin Exp Pharmacol Physiol Suppl. 1998; 25:S61–67. [PubMed: 9809195]

McKinley MJ, Pennington GL, Oldfield BJ. Anteroventral wall of the third ventricle and dorsal lamina terminalis: headquarters for control of body fluid homeostasis? Clin Exp Pharmacol Physiol. 1996; 23:271–281. [PubMed: 8717061]

Moga MM, Herbert H, Hurley KM, Yasui Y, Gray TS, Saper CB. Organization of cortical, basal forebrain, and hypothalamic afferents to the parabrachial nucleus in the rat. J Comp Neurol. 1990; 295:624–661. [PubMed: 1694187]

Moga MM, Moore RY. Organization of neural inputs to the suprachiasmatic nucleus in the rat. J Comp Neurol. 1997; 389:508–534. [PubMed: 9414010]

Moga MM, Saper CB. Neuropeptide-immunoreactive neurons projecting to the paraventricular hypothalamic nucleus in the rat. J Comp Neurol. 1994; 346:137–50. [PubMed: 7962708]

Mogenson GJ. Limbic-motor integration. Prog Psychobiol Physiol Psychol. 1987; 12:117–169.

Mogenson GJ, Swanson LW, Wu M. Evidence that projections from substantia innominata to zona incerta and mesencephalic locomotor region contribute to locomotor activity. Brain Res. 1985; 334:65–76. [PubMed: 3995314]

Monnier, M. Functions of the nervous system. Elsevier; Amsterdam: 1968.

Moore RY, Danchenko RL. Paraventricular-subparaventricular hypothalamic lesions selectively affect circadian function. Chronobiol Int. 2002; 19:345–360. [PubMed: 12025929]

Motohashi N, MacKenzie ET, Scatton B. Functional mapping of the effects of lesions of the habenular nuclei and their afferents in the rat. Brain Res. 1986; 397:265–278. [PubMed: 3801869]

Nogueira MI, de Rezende BD, do Vale LE, Bittencourt JC. Afferent connections of the caudal raphe pallidus nucleus in rats: a study using the fluorescent retrograde tracers fluorogold and true-blue. Anat Anz. 2000; 182:35–45.

Parkinson JA, Olmstead MC, Burns LH, Robbins TW, Everitt BJ. Dissociation in effects of lesions of the nucleus accumbens core and shell on appetitive Pavlovian approach behavior and the potentiation of conditioned reinforcement and locomotor activity by D-amphetamine. J Neurosci. 1999; 19:2401–2411. [PubMed: 10066290]

Pavcovich LA, Yang M, Miselis RR, Valentino RJ. Novel role for the pontine micturition center, Barrington's nucleus: evidence for coordination of colonic and forebrain activity. Brain Res. 1998; 784:355–361. [PubMed: 9518692]

Peterson R. Magnocellular neurosecretory centers in the rat hypothalamus. J Comp Neurol. 1966; 128:181–190. [PubMed: 4165735]

Petrovich GD, Setlow B, Holland PC, Gallagher M. Amygdalo-hypothalamic circuit allows learned cues to override satiety and promote eating. J Neurosci. 2002; 22:8748–8753. [PubMed: 12351750]

Petrovich GD, Swanson LW. Projections from the lateral part of the central amygdalar nucleus to the postulated fear conditioning circuit. Brain Res. 1997; 763:247–254. [PubMed: 9296566]

Phillipson OT. Afferent projections to the ventral tegmental area of Tsai and interfascicular nucleus: a horseradish peroxidase study in the rat. J Comp Neurol. 1979; 187:117–143. [PubMed: 489776]

Reynolds SM, Berridge KC. Positive and negative motivation in nucleus accumbens shell: bivalent rostrocaudal gradients for GABA-elicited eating, taste "liking"/"disliking" reactions, place preference/avoidance, and fear. J Neurosci. 2002; 22:7308–7320. [PubMed: 12177226]

Ricardo JA, Koh ET. Anatomical evidence of direct projections from the nucleus of the solitary tract to the hypothalamus, amygdala, and other forebrain structures in the rat. Brain Res. 1978; 153:1–26. [PubMed: 679038]

Risold PY, Swanson LW. Chemoarchitecture of the rat lateral septal nucleus. Brain Res Rev. 1997a; 24:91–113. [PubMed: 9385453]

Risold PY, Swanson LW. Connections of the rat lateral septal complex. Brain Res Rev. 1997b; 24:115–195. [PubMed: 9385454]

Risold PY, Thompson RH, Swanson LW. The structural organization of connections between hypothalamus and cerebral cortex. Brain Res Rev. 1997; 24:197–154. [PubMed: 9385455]

Saper CB. The central autonomic nervous system: conscious visceral perception and autonomic pattern generation. Ann Rev Neurosci. 2002; 25:433–469. [PubMed: 12052916]

Saper CB, Chou TC, Scammell TE. The sleep switch: hypothalamic control of sleep and wakefulness. Trends Neurosci. 2001; 24:726–731. [PubMed: 11718878]

Saper CB, Loewy AD, Swanson LW, Cowan WM. Direct hypothalamo-autonomic connections. Brain Res. 1976; 117:305–312. [PubMed: 62600]

Satoh K, Shimizu M, Tohyama M, Maeda T. Localization of the micturition reflex center at dorsolateral pontine tegmentum of the rat. Neurosci Lett. 1978; 8:27–33. [PubMed: 19605144]

Sawchenko PE, Swanson LW. A method for tracing biochemically defined pathways in the central nervous system using combined fluorescence retrograde transport and immunohistochemical techniques. Brain Res. 1981; 210:31–51. [PubMed: 6164442]

Sawchenko PE, Swanson LW. The organization of forebrain afferents to the paraventricular and supraoptic nuclei of the rat. J Comp Neurol. 1983; 218:121–144. [PubMed: 6886068]

Scalia F, Winans S. The differential projections of the olfactory bulb and accessory olfactory bulb in mammals. J Comp Neurol. 1975; 161:31–56. [PubMed: 1133226]

Scammell TE, Estabrooke IV, McCarthy MT, Chemelli RM, Yanagisawa M, Miller MS, Saper CB. Hypothalamic arousal regions are activated during modafinil-induced wakefulness. J Neurosci. 2000; 20:8620–8628. [PubMed: 11069971]

Sherin JE, Elmquist JK, Torrealba F, Saper CB. Innervation of histaminergic tuberomammillary neurons by GABAergic and galaninergic neurons in the ventrolateral preoptic nucleus of the rat. J Neurosci. 1998; 18:4705–21. [PubMed: 9614245]

Sherin JE, Shiromani PJ, McCarley RW, Saper CB. Activation of ventrolateral preoptic neurons during sleep. Science. 1996; 271:216–219. [PubMed: 8539624]

Simerly RB, Swanson LW. The organization of neural inputs to the medial preoptic nucleus of the rat. J Comp Neurol. 1986; 246:312–342. [PubMed: 3517086]

Simerly RB, Swanson LW. Projections of the medial preoptic nucleus: a Phaseolus vulgaris-leucoagglutinin anterograde tract-tracing study in the rat. J Comp Neurol. 1988; 270:209–242. [PubMed: 3259955]

Simerly RB, Swanson LW, Gorski RA. Demonstration of a sexual dimorphism in the distribution of serotonin-immunoreactive fibers in the medial preoptic nucleus of the rat. J Comp Neurol. 1984; 225:151–166. [PubMed: 6373846]

Smith JE, Jansen AS, Gilbey MP, Loewy AD. CNS cell groups projecting to sympathetic outflow of tail artery: neural circuits involved in heat loss in the rat. Brain Res. 1998; 786:153–164. [PubMed: 9554992]

Spencer SJ, Buller KM, Day TA. Medial prefrontal cortex control of the paraventricular hypothalamic nucleus response to psychological stress: possible role of the bed nucleus of the stria terminalis. J Comp Neurol. 2005; 481:363–376. [PubMed: 15593338]

Stratford TR, Kelley AE. Evidence of a functional relationship between the nucleus accumbens shell and lateral hypothalamus subserving the control of feeding behavior. J Neurosci. 1999; 19:11040–11048. [PubMed: 10594084]

Sun N, Cassell MD. Intrinsic GABAergic neurons in the rat central extended amygdala. J Comp Neurol. 1993; 330:381–404. [PubMed: 8385679]

Sunn N, McKinley MJ, Oldfield BJ. Circulating angiotensin II activates neurones in circumventricular organs of the lamina terminalis that project to the bed nucleus of the stria terminalis. J Neuroendocrinol. 2003; 15:725–31. [PubMed: 12834432]

Swanson LW. An autoradiographic study of the efferent connections of the preoptic region in the rat. J Comp Neurol. 1976; 167:227–256. [PubMed: 819466]

Swanson, LW. Organization of mammalian neuroendocrine system. In: Bloom, FE., editor. Handbook of physiology, the nervous system, IV. Waverly Press; Baltimore: 1986. p. 317-363.

Swanson, LW. The hypothalamus. In: Björklund, A.; Hökfelt, T.; Swanson, LW., editors. Handbook of chemical neuroanatomy, Vol. 5 Integrated systems of the CNS, Part I. Elsevier; Amsterdam: 1987. p. 1-124.

Swanson, LW. Brain maps: structure of the rat brain. 2nd ed.. Elsevier; Amsterdam: 1998-1999.

Swanson LW. Cerebral hemisphere regulation of motivated behavior. Brain Res. 2000; 886:113–164. [PubMed: 11119693]

Swanson LW. The amygdala and its place in the cerebral hemisphere. Ann NY Acad Sci. 2003; 985:174–184. [PubMed: 12724158]

Swanson, LW. Brain maps: structure of the rat brain. 3rd ed.. Elsevier; Amsterdam: 2004.

Swanson LW, Cowan WM. The connections of the septal region in the rat. J Comp Neurol. 1979; 186:621–656. [PubMed: 15116692]

Swanson LW, Hartman BK. The central adrenergic system. An immunofluorescence study of the location of cell bodies and their efferent connections in the rat utilizing dopamine-beta-hydroxylase as a marker. J Comp Neurol. 1975; 163:467–505. [PubMed: 1100685]

Swanson LW, Kuypers HGJM. A direct projection from the ventromedial nucleus and retrochiasmatic area of the hypothalamus to the medulla and spinal cord of the rat. Neurosci Lett. 1980a; 17:307–312. [PubMed: 7052476]

Swanson LW, Kuypers HGJM. The paraventricular nucleus of the hypothalamus: cytoarchitectonic subdivisions and organization of projections to the pituitary, dorsal vagal complex, and spinal

cord as demonstrated by retrograde fluorescence double-labeling methods. J Comp Neurol. 1980b; 194:555–570. [PubMed: 7451682]

Swanson LW, Lind RW. Neural projections subserving the initiation of a specific motivated behavior in the rat: new projections from the subfornical organ. Brain Res. 1986; 379:399–403. [PubMed: 3742231]

Swanson LW, McKellar S. The distribution of oxytocin- and neurophysin-stained fibers in the spinal cord of the rat and monkey. J Comp Neurol. 1979; 188:87–106. [PubMed: 115910]

Swanson LW, Mogenson GJ, Gerfen CR, Robinson P. Evidence for a projection from the lateral preoptic area and substantia innominata to the 'mesencephalic locomotor region' in the rat. Brain Res. 1984; 295:161–178. [PubMed: 6201228]

Swanson LW, Petrovich GD. What is the amygdala? Trends Neurosci. 1998; 21:323–331. [PubMed: 9720596]

Swanson LW, Sawchenko PE, Rivier J, Vale WW. Organization of ovine corticotropin-releasing factor immunoreactive cells and fibers in the rat brain: an immunohistochemical study. Neuroendocrinol. 1983; 36:165–186.

Taheri S, Zeitzer JM, Mignot E. The role of hypocretins (orexins) in sleep regulation and narcolepsy. Ann Rev Neurosci. 2002; 25:283–313. [PubMed: 12052911]

Thompson RH, Swanson LW. Structural characterization of a hypothalamic visceromotor pattern generator network. Brain Res Rev. 2003; 41:153–202. [PubMed: 12663080]

Tzschentke TM, Schmidt WJ. Functional relationship among medial prefrontal cortex, nucleus accumbens, and ventral tegmental area in locomotion and reward. Crit Rev Neurobiol. 2000; 14:131–142. [PubMed: 11513242]

Valentino RJ, Kosboth M, Colflesh M, Miselis RR. Transneuronal labeling from the rat distal colon: anatomic evidence for regulation of distal colon function by a pontine corticotropin-releasing factor system. J Comp Neurol. 2000; 417:399–414. [PubMed: 10701863]

Valentino RJ, Page ME, Luppi PH, Zhu Y, Van Bockstaele E, Aston-Jones G. Evidence for widespread afferents to Barrington's nucleus, a brainstem region rich in corticotropin-releasing hormone neurons. Neuroscience. 1994; 62:125–143. [PubMed: 7816195]

Van Bockstaele EJ, Aston-Jones G, Pieribone VA, Ennis M, Shipley MT. Subregions of the periaqueductal gray topographically innervate the rostral ventral medulla in the rat. J Comp Neurol. 1991; 309:305–327. [PubMed: 1717516]

van der Kooy D, Koda LY, McGinty JF, Gerfen CR, Bloom FE. The organization of projections from the cortex, amygdala, and hypothalamus to the nucleus of the solitary tract in rat. J Comp Neurol. 1984; 224:1–24. [PubMed: 6715573]

Vertes RP. A PHA-L analysis of ascending projections of the dorsal raphe nucleus in the rat. J Comp Neurol. 1991; 313:643–668. [PubMed: 1783685]

Vertes RP. PHA-L analysis of projections from the supramammillary nucleus in the rat. J Comp Neurol. 1992; 326:595–622. [PubMed: 1484125]

Vertes RP, Crane AM. Descending projections of the posterior nucleus of the hypothalamus: Phaseolus vulgaris-leucoagglutinin analysis in the rat. J Comp Neurol. 1996; 374:607–631. [PubMed: 8910738]

Vertes RP, Kocsis B. Brainstem-diencephalo-septohippocampal systems controlling the theta rhythm of the hippocampus. Neuroscience. 1997; 81:893–926. [PubMed: 9330355]

Watts AG. Understanding the neural control of ingestive behaviors: helping to separate cause from effect with dehydration-associated anorexia. Horm Behav. 2000; 37:261–283. [PubMed: 10860672]

Watts AG. Neuropeptides and the integration of motor responses to dehydration. Ann Rev Neurosci. 2001; 24:357–384. [PubMed: 11283315]

Watts AG, Sanchez-Watts G, Kelly AB. Distinct patterns of neuropeptide gene expression in the lateral hypothalamic area and arcuate nucleus are associated with dehydration-induced anorexia. J Neurosci. 1999; 19:6111–6121. [PubMed: 10407047]

Watts AG, Swanson LW. Efferent projections of the suprachiasmatic nucleus: II. Studies using retrograde transport of fluorescent dyes and simultaneous peptide immunohistochemistry in the rat. J Comp Neurol. 1987; 258:230–252. [PubMed: 2438309]

Watts AG, Swanson LW, Sanchez-Watts G. Efferent projections of the suprachiasmatic nucleus: I. Studies using anterograde transport of Phaseolus vulgaris-leucoagglutinin in the rat. J Comp Neurol. 1987; 258:204–229. [PubMed: 3294923]

Westerhaus MJ, Loewy AD. Sympathetic-related neurons in the preoptic region of the rat identified by viral transneuronal labeling. J Comp Neurol. 1999; 414:361–378. [PubMed: 10516602]

Willie JT, Chemelli RM, Sinton CM, Yanagisawa M. To eat or to sleep? Orexin in the regulation of feeding and wakefulness. Ann Rev Neurosci. 2001; 24:429–458. [PubMed: 11283317]

Wilson C, Nomikos GG, Collu M, Fibiger HC. Dopaminergic correlates of motivated behavior: importance of drive. J Neurosci. 1995; 15:5169–5178. [PubMed: 7623143]

Wise RA. Brain reward circuitry: insights from unsensed incentives. Neuron. 2002; 36:229–240. [PubMed: 12383779]

Yamamoto T, Matsuo R, Kiyomitsu Y, Kitamura R. Response properties of lateral hypothalamic neurons during ingestive behavior with special reference to licking of various taste solutions. Brain Res. 1989; 481:286–297. [PubMed: 2720381]
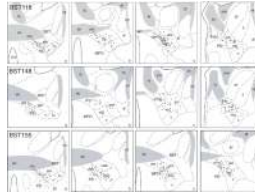
Fig. 1.
Camera lucida plots showing the distribution of PHAL-labeled neurons (black dots) in transverse histological sections through three injection sites centered in the BSTdm (experiments BST116, BST148, and BST155). In each row, drawings are arranged from rostral (a) to caudal (d).

Fig. 2.
Brightfield photomicrographs to show the appearance of a PHAL injection site centered in the BSTdm (A, experiment BST116) and its caudally adjacent Nissl-stained transverse section (B). Photomicrographs correspond approximately to the level in Fig. 4I. Scale bars = 200 μm.
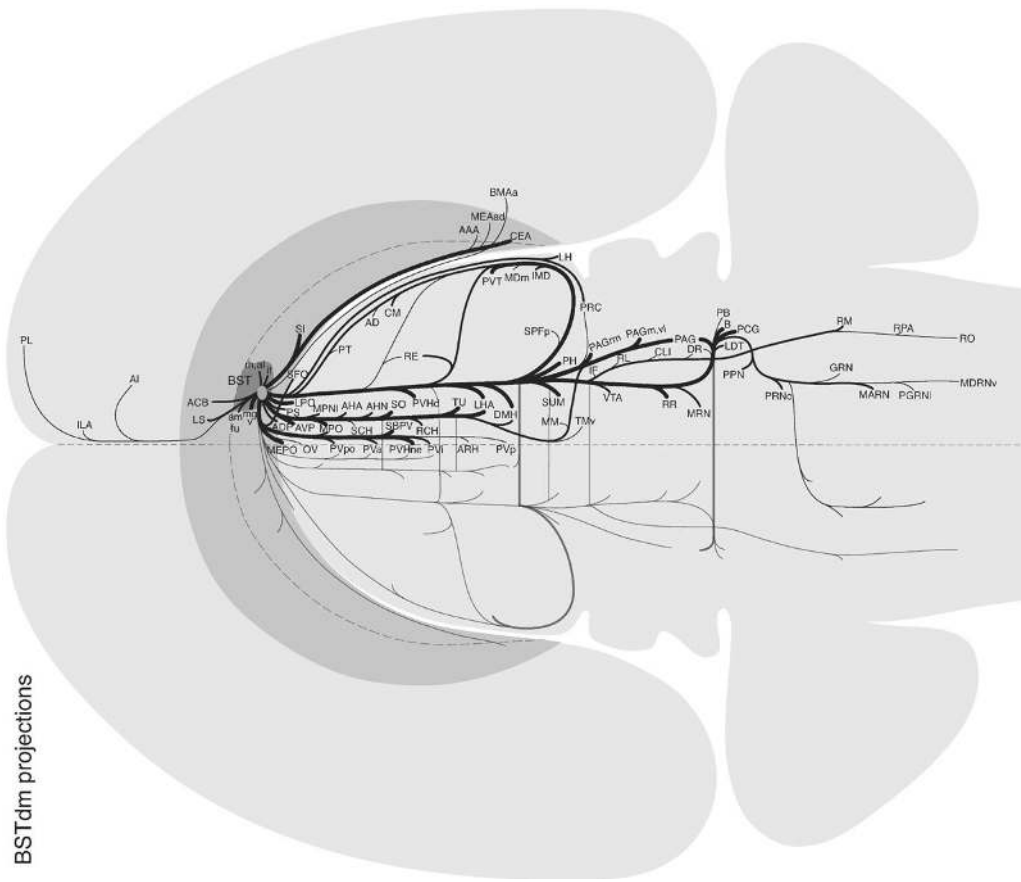
BSTdm projections

Fig. 3.
This summary diagram indicates the general organization of projections from the BSTdm.
The relative size of each pathway is roughly proportional to the thickness of the line
representing it. The flatmap is based on Swanson (2004).
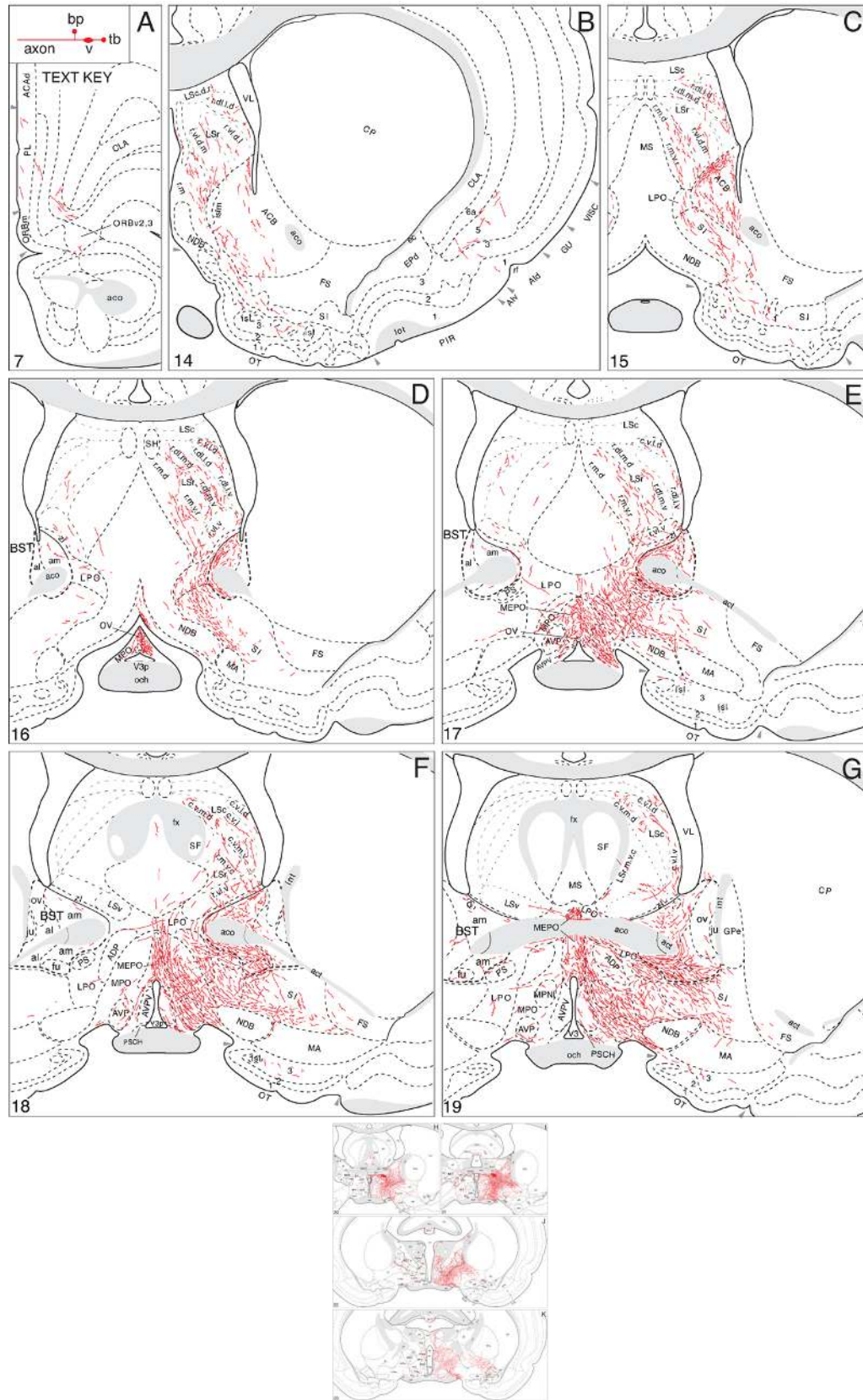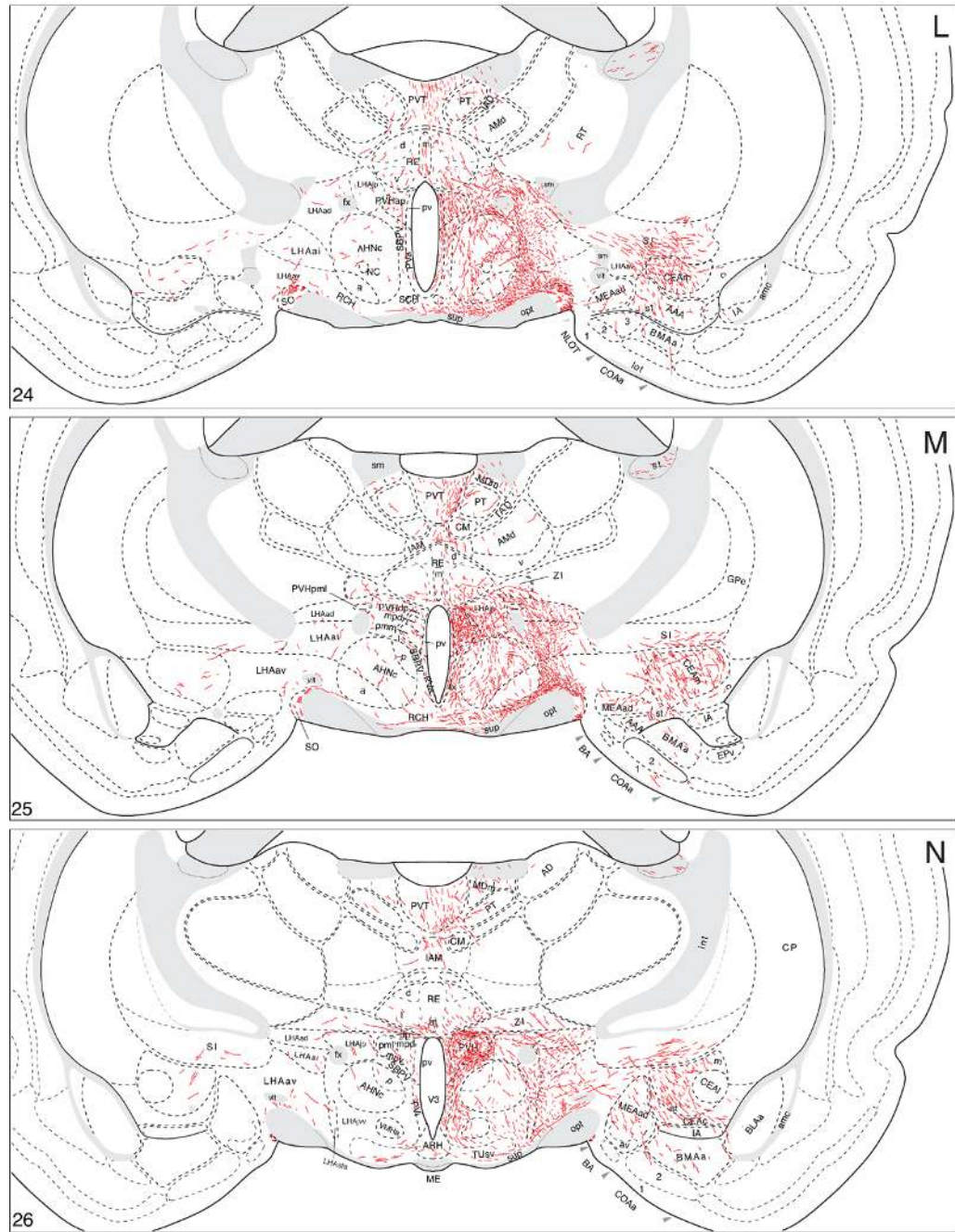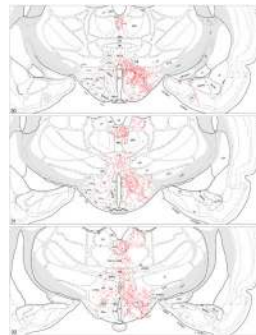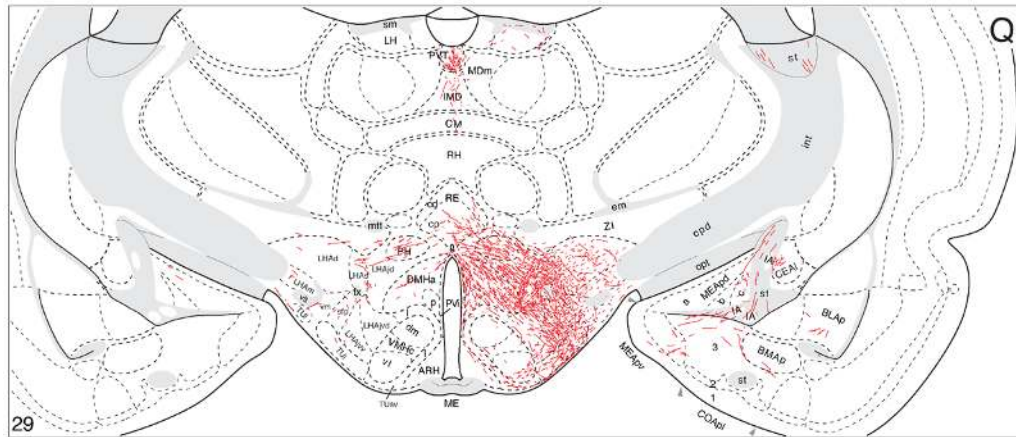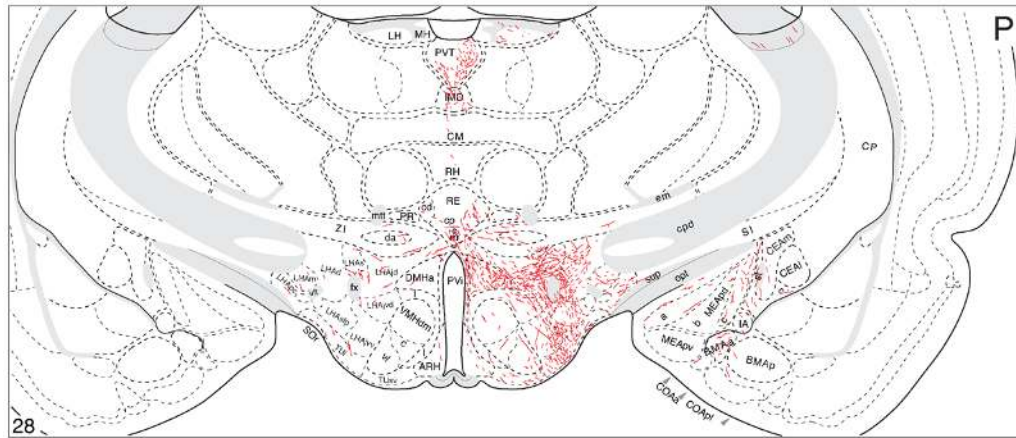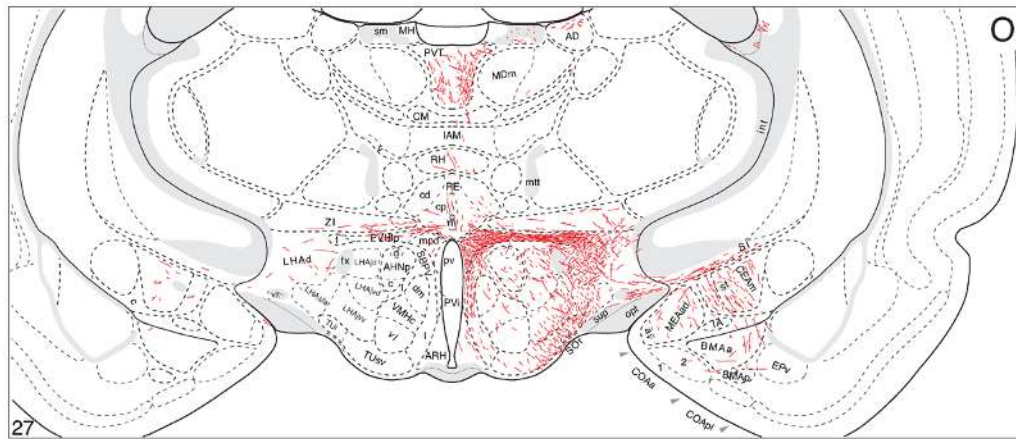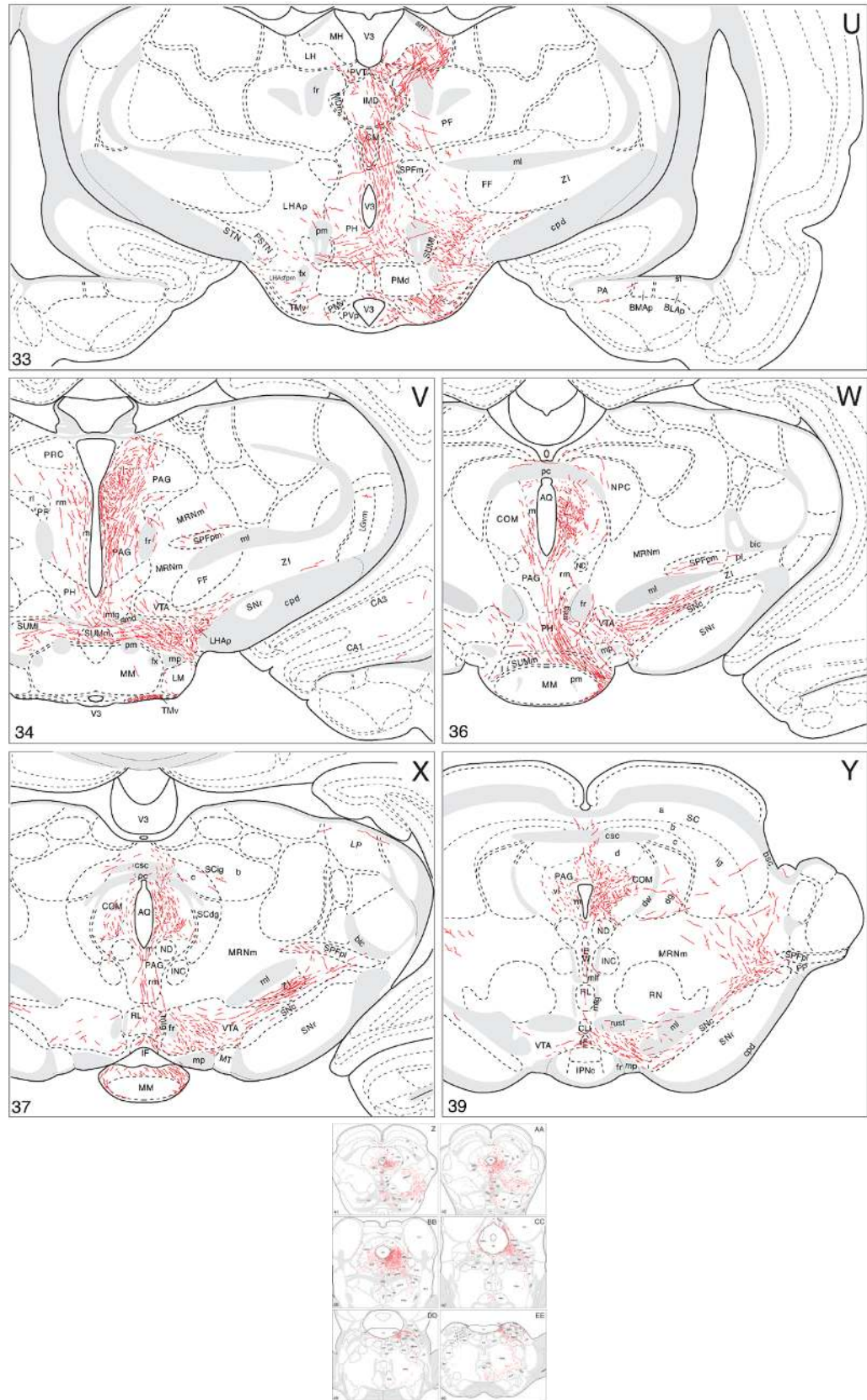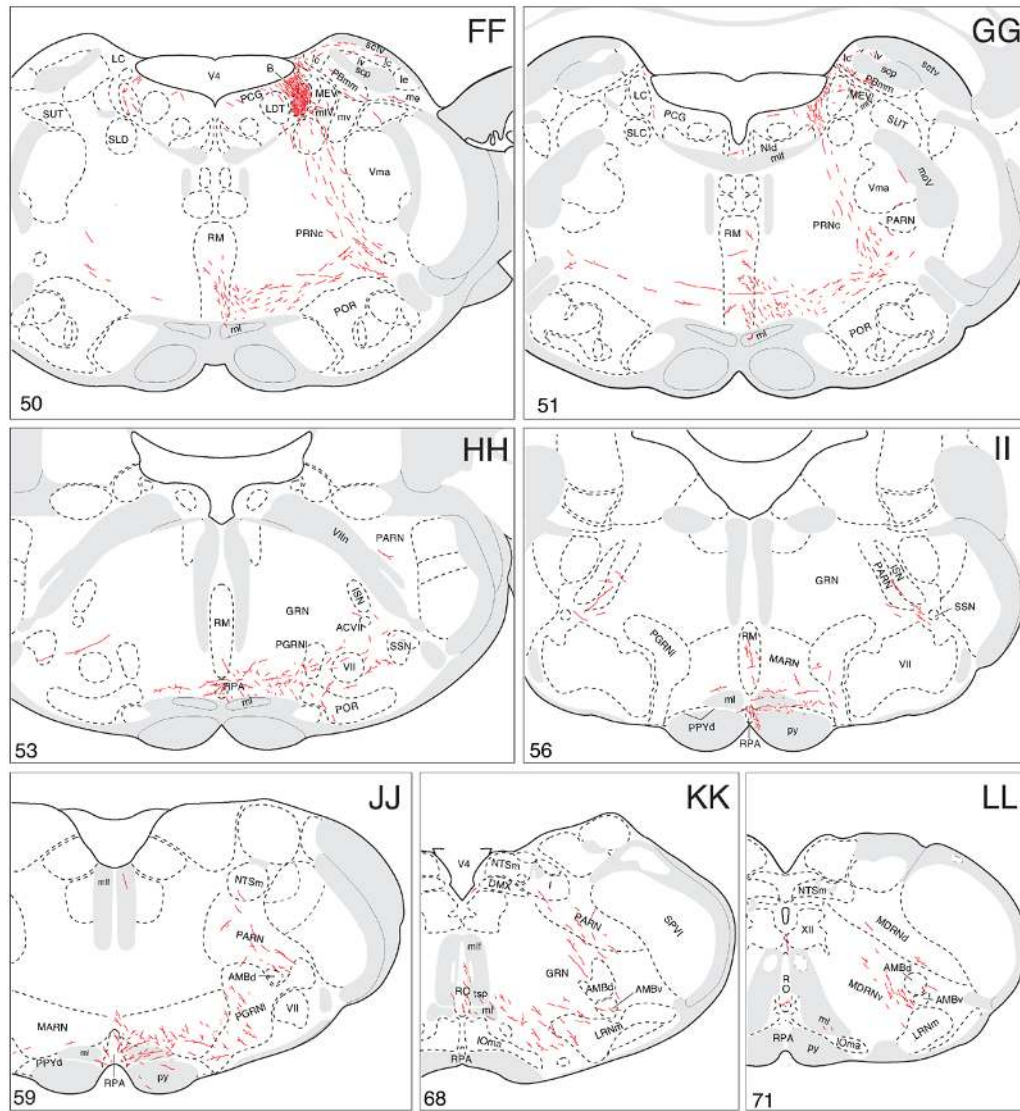
Fig. 4.
A summary of BSTdm pathways and terminal fields. The distribution of PHAL-labeled axons (thin red lines) in experiment BST116 was plotted onto a series of standard or reference drawings of the rat brain derived from an atlas (Swanson, 2004), and arranged from rostral (A) to caudal (LL). The red areas centered in the BSTdm at levels H and I indicate the injection site (see Figs. 1 and 2). The key in the upper left corner of level A illustrates the meaning of terms used in the text to describe PHAL-labeled axons. Boutons-of-passage (bp) and terminal boutons (tb) are also referred to simply as terminals, whereas varicosities (v) may or may not form synapses (see Swanson, 2004). The scale of the drawings themselves is too small to illustrate these features. The number in the lower left corner of each drawing refers to the corresponding Atlas Level.
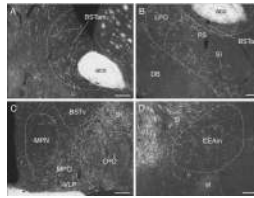
Fig. 5.
Darkfield photomicrographs show the appearance of PHAL labeling in rostral regions of the BST anteromedial area (A; about Fig. 4D); in ventral regions of the BST anteromedial area, rostral region of the lateral preoptic area, and rostral region of the substantial innominata (B; about Fig. 4E); in the ventral nucleus of the BST, dorsal regions of the substantial innominata (SI), and the medial and lateral preoptic areas (C; about Fig. 4H); and in the medial part of the central amygdalar nucleus (D; about Fig. 4M). All scale bars = 200 μm.
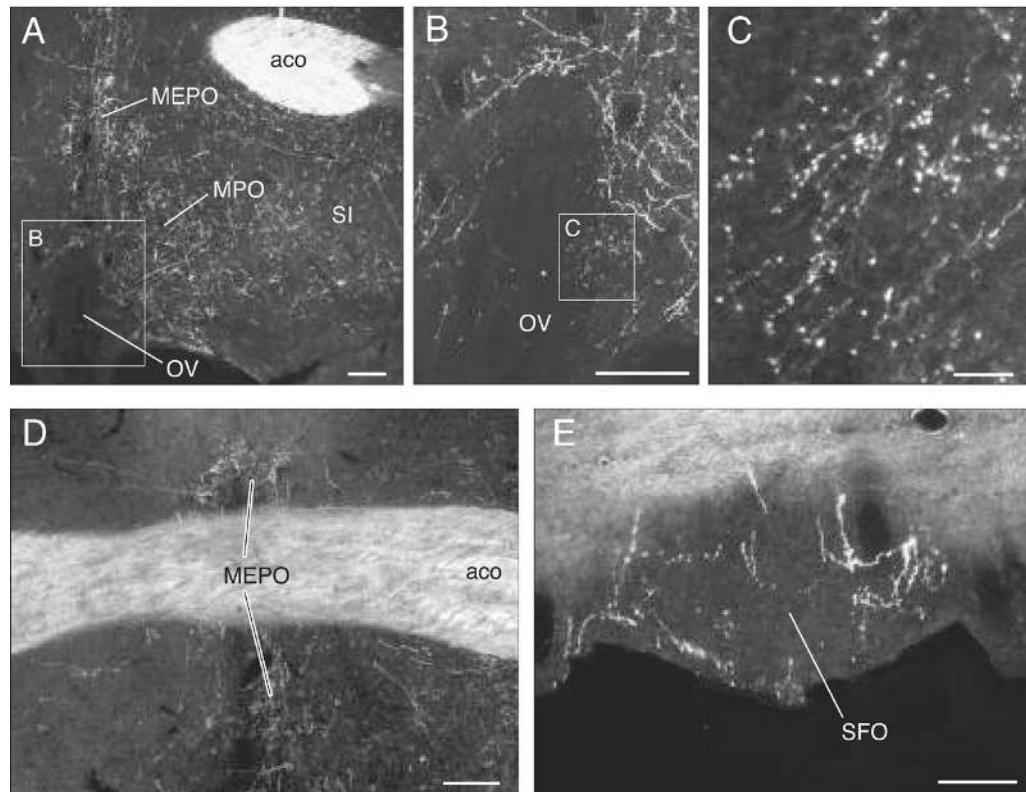
Fig. 6.
Darkfield photomicrographs show the appearance of PHAL labeling in the median preoptic nucleus (A,D; about Figs. 4E and 4G, respectively), vascular organ of lamina terminalis (A-C; about Fig. 4E), and subfornical organ (E; about Fig. 4K). The rectangle in A outlines the field enlarged in B, and the rectangle in B outlines the field enlarged even more in C. Note PHAL-labeled boutons immediately surrounding the vascular organ (B,C) and in peripheral regions of subfornical organ (E). Scale bars = 200 μm in A,B, and D; 25 μm in C; and 100 μm in E.
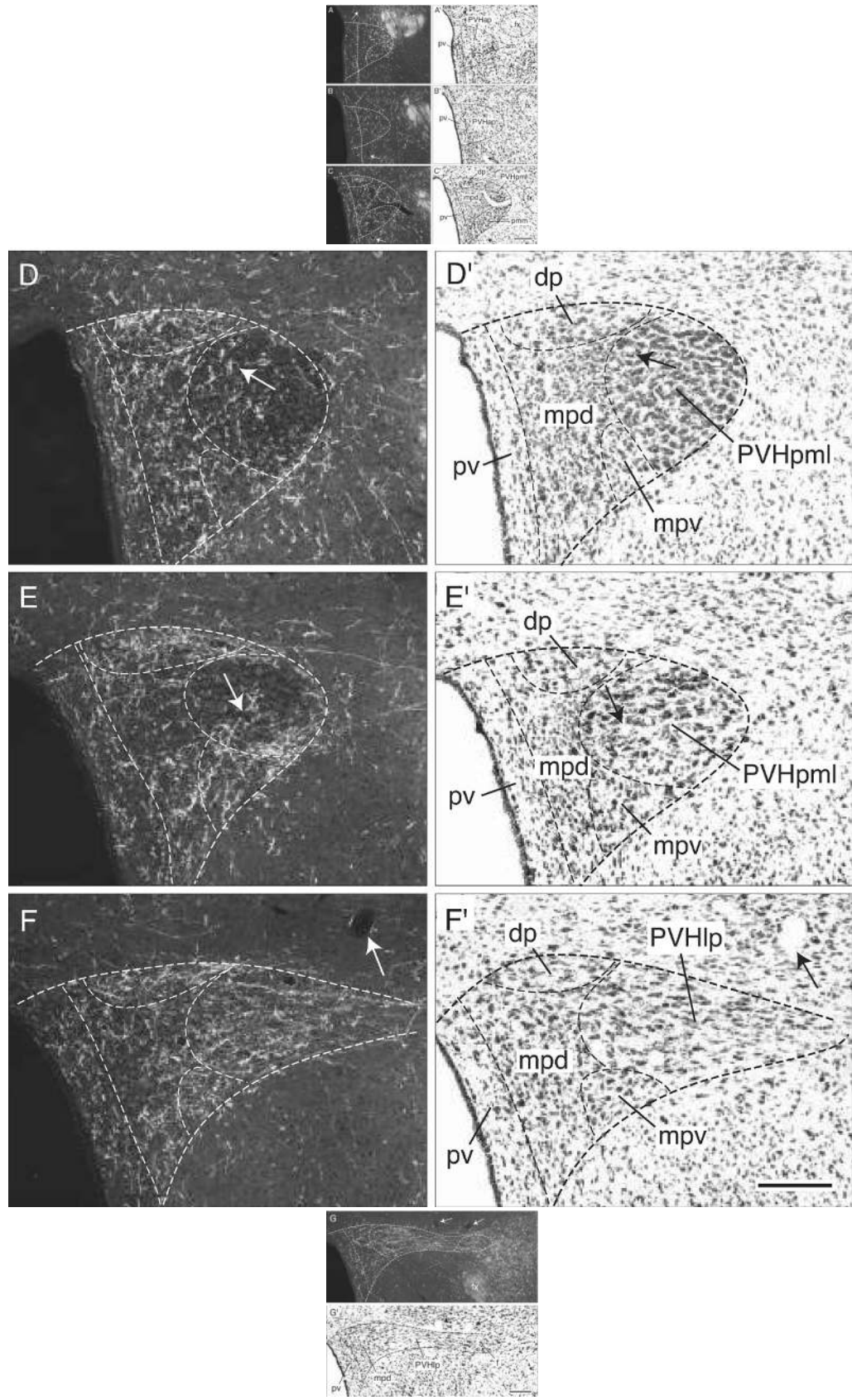
Fig. 7.
Darkfield photomicrographs showing the appearance of PHAL-labeled axons from the BSTdm (experiment BST116) in transverse histological sections through the paraventricular hypothalamic nucleus from rostral to caudal (A-G; about Fig. 4J-O). For subdivisions of the paraventricular nucleus, see the corresponding caudally adjacent thionin-stained transverse sections (A'-G'). Arrows point to the same blood vessels in the pairs of photomicrographs. Scale bars = 150 μm.
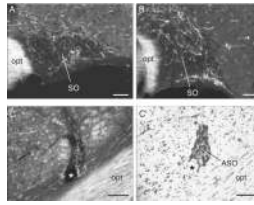
Fig. 8.
Darkfield photomicrographs show the appearance of PHAL labeling in two different levels of the supraoptic nucleus (A and B), and in the accessory supraoptic nucleus (C). For cytoarchitectonic character of the accessory supraoptic nucleus, see the caudally adjacent thionin-stained transverse section (C'). Asterisks in C and C' indicate same blood vessels. Parts A, B, and C correspond approximately to Fig. 4 levels K, L, and N, respectively. Scale bar = 200 μm in A,B; 150 μm in C.
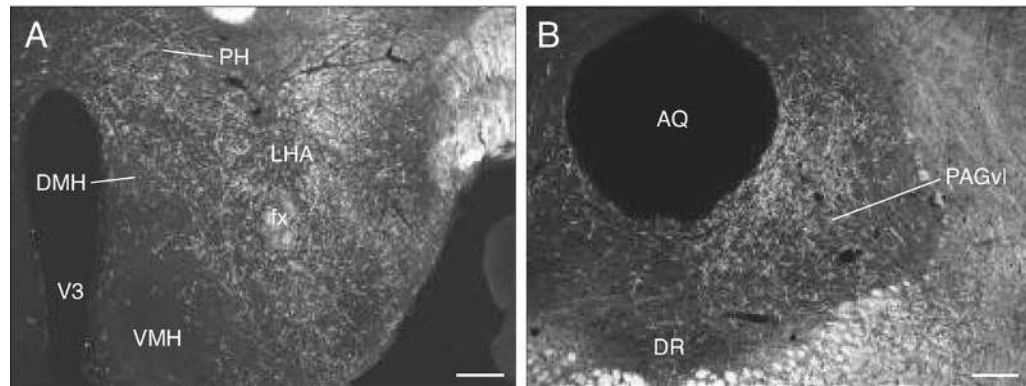
Fig. 9.
Darkfield photomicrographs show the appearance of PHAL labeling in the lateral hypothalamic area, dorsomedial hypothalamic nucleus, and rostral posterior hypothalamic nucleus (A; about Fig. 4Q), and in the ventrolateral division of the periaqueductal gray (B; about Fig. 4BB). Scale bars = 200 μm.
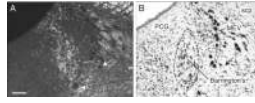
Fig. 10.
Darkfield photomicrographs show the appearance of PHAL labeling in Barrington's nucleus (A; about Fig. 4FF), along with the caudally adjacent thionin-staining section (B). Arrows point to the same blood vessels in the photomicrographs. Scale bar = 100 μm.
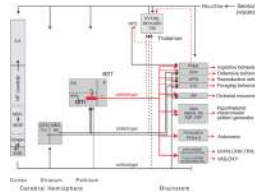
Fig. 11.
Schematic overview showing how the BSTdm participates in a basic triple descending projection from the three major parts of the cerebral hemisphere to the brainstem motor system, with a thalamocortical feedback loop (dashed lines). Direct outputs of the BSTdm itself are indicated in red. References for the circuitry are provided in the Discussion section, except as noted below. For clarity, details of ascending inputs to cerebral cortical areas, interconnections between cortical areas, and the descending targets of each indicated cortical area, are not illustrated (they are reviewed in Swanson, 2000; Dong et al., 2001a; Dong and Swanson, 2003a). For the same reason, projections from the BSTdm to other parts of the striatum (nucleus accumbens and lateral septal nucleus) and pallidum (substantia innominata), and to the behavioral state system (especially the supramammillary and tuberomammillary nuclei) also are not illustrated. Along with contributions from the adjacent magnocellular and ventral nuclei of the BST (see Dong and Swanson 2005a), this differentiation of the cortico-striatopallidal system has a uniquely direct influence in pelvic functions. Diagram adapted from Figure 32C in Swanson (2000).